

Research Report: Regular Manuscript

Long Latency Responses to a Mechanical Perturbation of the Index Finger have a Spinal Component

<https://doi.org/10.1523/JNEUROSCI.1901-19.2020>

Cite as: J. Neurosci 2020; 10.1523/JNEUROSCI.1901-19.2020

Received: 27 July 2019

Revised: 21 January 2020

Accepted: 25 January 2020

This Early Release article has been peer-reviewed and accepted, but has not been through the composition and copyediting processes. The final version may differ slightly in style or formatting and will contain links to any extended data.

Alerts: Sign up at www.jneurosci.org/alerts to receive customized email alerts when the fully formatted version of this article is published.

Copyright © 2020 Soteropoulos and Baker

This is an open-access article distributed under the terms of the Creative Commons Attribution 4.0 International license, which permits unrestricted use, distribution and reproduction in any medium provided that the original work is properly attributed.

Long Latency Responses to a Mechanical Perturbation of the Index Finger have a Spinal Component

Demetris S. Soteropoulos & Stuart N. Baker

Institute of Neuroscience, Newcastle University, Newcastle, NE2 4HH, UK

Abbreviated title: Spinal responses to finger perturbation.

Corresponding author:

Demetris Soteropoulos
Demetris.soteropoulos@ncl.ac.uk
Lecturer in Motor Systems Neuroscience
Institute of Neuroscience
Newcastle University
United Kingdom

Number of figures: 16
Number of words in the Abstract: 242
Number of words in the Introduction: TBC
Number of words in the Discussion: TBC

Acknowledgements & Funding

The authors would like to thank Elizabeth Williams and Terri Jackson for assistance with animal training and data collection. This work was funded by the MRC and the Wellcome Trust.

Conflict of Interest: The authors are not aware of any conflict of interest.

35 **Abstract**

36 In an uncertain external environment, the motor system may need to respond rapidly to an
37 unexpected stimulus. Limb displacement causes muscle stretch; the corrective response has multiple
38 activity bursts, which are suggested to originate from different parts of the neuraxis. The earliest
39 response is so fast, it can only be produced by spinal circuits; this is followed by slower components
40 thought to arise from primary motor cortex (M1) and other supraspinal areas. Spinal cord (SC)
41 contributions to the slower components are rarely considered. To address this, we recorded neural
42 activity in M1 and the cervical SC during a visuomotor tracking task, in which two female macaque
43 monkeys moved their index finger against a resisting motor to track an on-screen target. Following
44 the behavioral trial, an increase in motor torque rapidly returned the finger to its starting position
45 (lever velocity $>200^{\circ}/s$). Many cells responded to this passive mechanical perturbation (M1: 148/211
46 cells, 70%; SC: 67/119 cells, 56%). The neural onset latency was faster for SC compared to M1 cells
47 (21.7 ± 11.2 ms vs 25.5 ± 10.7 ms respectively, mean \pm SD). Using spike triggered averaging, some cells
48 in both regions were identified as likely premotor cells, with monosynaptic connections to
49 motoneurons. Response latencies for these cells were compatible with a contribution to the muscle
50 responses following the perturbation. Comparable fractions of responding neurons in both areas
51 were active up to 100 ms after the perturbation, suggesting that both SC circuits and supraspinal
52 centers could contribute to later response components.

53 **Significance Statement**

54 Following a limb perturbation, multiple reflexes help to restore limb position. Given conduction
55 delays, the earliest part of these reflexes can only arise from spinal circuits. By contrast, long latency
56 reflex components are typically assumed to originate from supraspinal centers. We recorded from
57 both spinal and motor cortical cells in monkeys responding to index finger perturbations. Many
58 spinal interneurons, including those identified as projecting to motoneurons, responded to the
59 perturbation; the timing of responses was compatible with a contribution to both short- and long-
60 latency reflexes. We conclude that spinal circuits also contribute to long latency reflexes in distal and
61 forearm muscles, alongside supraspinal regions such as the motor cortex and brainstem.

62 **Introduction**

63 The spinal cord (SC) is often considered to be the epicenter of limb reflexes, as it contains the
64 necessary neural circuits for mediating a varied repertoire of very fast responses to an external
65 stimulus. This is exemplified by the classical stretch reflex, whereby a mechanical stimulus causes

66 the rapid lengthening of a muscle, which in turn causes the same muscle to contract with an onset
67 too fast to be mediated through any system except the SC.

68 Muscle responds to stretch with multiple bursts of activity. The earliest component, referred to as
69 the short latency response (SLR), is mediated through fast Group Ia spindle afferents with
70 conduction velocities around 85 m/s. Primary spindle afferents are particularly sensitive to rapid
71 changes in muscle length (Matthews 1972), are reliably activated during a mechanical perturbation
72 and have direct and potent monosynaptic connections onto motoneurons (Jack et al. 1971;
73 Landgren et al. 1962; Mendell and Henneman 1968). After the SLR contributions from the SC are
74 typically considered to be over, any later muscle activity, usually termed the Long Latency Response
75 (LLR, also used as such in our paper), is thought to be mediated through supraspinal systems.

76 One such supraspinal system is the primary motor cortex (M1). Neurons in M1 respond to peripheral
77 stimulation (Lemon and Porter 1976a; b) with a short delay, and in turn there are numerous
78 projections from M1 back down to the SC. In primates, some M1 cells directly contact motoneurons
79 (Lemon et al. 1998; Maier et al. 1993). These cortico-motoneuronal (CM) cells respond to
80 mechanical perturbations in distal joints at delays compatible with a contribution to the LLR in
81 monkey forearm muscles (Cheney and Fetz 1984). The transcortical component of the LLR probably
82 partly explains its sensitivity to varying task demands (Omrani et al. 2014; Pruszynski 2014;
83 Pruszynski et al. 2014). Other possible contributors include subcortical areas with their own
84 descending pathways to the SC, such as the brainstem reticular formation (RF) and red nucleus
85 (Herter et al. 2015; Soteropoulos et al. 2012).

86 Given the involvement of spinal neuronal circuits in complex motor actions, spinal contributions to
87 components later than the monosynaptic stretch reflex would be to be expected (see Fig 1). Indeed,
88 muscle responses at LLR delays survive interruption of the transcortical route in both monkeys and
89 cats (Ghez and Shinoda 1978; Miller and Brooks 1981; Tracey et al. 1980). Similar evidence also
90 exists in humans with spinal cord injury (Roby-Brami and Bussel 1987). Many spinal interneurons in
91 the intermediate layers of the SC receive sensory inputs from several afferent classes (Brown and
92 Fyffe 1979; Brown and Fyffe 1978; Fyffe 1979; Jankowska and Edgley 2010; Jankowska and McCrea
93 1983; Jankowska et al. 1981; Lundberg 1979b), and many in turn also provide a potent source of
94 inputs to motoneurons (Fetz et al. 1996; Takei and Seki 2010; 2013; Williams et al. 2010).

95 Disentangling the specific contribution of afferents inputs through spinal interneurons is hard to do
96 in man, particularly for the upper limb (but see Pierrot-Deseilligny and Burke 2012). Manipulations
97 such as peripheral cooling of the arm (Matthews 1989) and pharmacological interventions using
98 tizanidine (Lourenco et al. 2006; Marque et al. 2005; Meskers et al. 2010) have shown a potential

99 Group II involvement in the LLR, but results have not been consistent (see Kurtzer et al. 2018). Other
100 studies provide support for a cutaneous afferent contribution to the LLR (Corden et al. 2000).

101 In order to assess the importance of spinal circuits to the LLR, it is necessary to show that spinal
102 circuits are activated following a perturbation during behavior, and to relate the onset and duration
103 of the SC responses to that of the muscles. In the reported experiments, we recorded the responses
104 of SC cells to a mechanical perturbation of the index finger in the awake behaving monkey, and
105 compared their firing with that of M1 cells. A substantial fraction of SC neurons responded to index
106 finger perturbations; the timing of discharge modulation was consistent with a contribution to both
107 early and late components of the muscle response.

108 **Methods**

109 All animal procedures were performed under UK Home Office regulations in accordance with the
110 Animals (Scientific Procedures) Act (1986) and were approved by the relevant Local Research Ethics
111 Committee. Experiments were carried out on two adult female purposed bred macaque monkeys
112 (*Macaca mulatta*). Animals were pair housed, and had ad libitum access to water at all times. Food
113 access was restricted during training and recordings but was ad libitum during the weekend. If the
114 number of rewards taken during recordings fell below a threshold level for two consecutive days,
115 animals were given ad libitum access to food on the second day.

116

117 **Behavioral task**

118 The task has been described previously (Soteropoulos et al. 2012; Williams et al. 2009; 2010) but
119 briefly animals were trained to carry out a slow index finger movement using visual feedback. The
120 hand, and digits 1 and 3–5, rested within a padded pocket which constrained movements in all
121 directions while the index finger was used to carry out flexion/extension movements through
122 movements across the metacarpophalangeal joint. The index finger pressed on a lever attached to
123 the shaft of a torque motor and optical encoder, mounted approximately coaxially with the
124 metacarpophalangeal joint. The target appeared at a stationary position (HOLD 1, 1 s), moved with a
125 constant velocity of 12°s^{-1} (movement period, RAMP) for 1 s, and then remained stationary for a
126 further 1 s (HOLD 2). Movements were either in the extension or flexion direction, chosen randomly;
127 the HOLD 1 and HOLD 2 displacements required flexion by 12° or 24° from the neutral position. The
128 lever was attached to a motor which simulated a spring load (torque for initial lever movement, 26.4
129 mN m; spring constant, 1.8 mN m deg^{-1}). Force on the lever was always in a direction to oppose
130 finger flexion. Deviations from the target (typically $> 1.4^\circ$) resulted in an error signal and the trial was

131 terminated with no reward. At the end of a correct trial, or after an error during the trial, the lever
 132 was rapidly (peak velocity typically in excess of 100 °/s) returned to the start position by increasing
 133 the torque to the motor. If the trial was successful, the monkey was given a food/liquid reward. The
 134 working arm was gently supported in a sleeve to prevent proximal movements, while the
 135 contralateral arm was not restrained.

136 **Surgery and implants**

137 Following behavioral training, monkeys were implanted with a stainless steel headpiece to allow
 138 atraumatic head fixation. Recording chambers were over the primary motor cortex (chamber center
 139 12mm anterior to the interaural line and 18mm lateral to midline) to allow single unit recordings
 140 from this area. Animals were prepared for EMG recording by implantation with up to 10 epimysial
 141 patch electrodes, sutured to hand and forearm muscles (see below for list of muscles). Wires from
 142 these electrodes led subcutaneously to a connector mounted on the animal's back. Following
 143 recordings from M1 and the RF (reticular data is not part of this paper), a spinal chamber was
 144 implanted over the cervical SC, involving fusion of vertebrae from C4 to T2 (Williams et al. 2010).

145 To allow antidromic identification of corticospinal neurons (pyramidal tract neurons, PTNs), stainless
 146 steel stimulating electrodes insulated with parylene (MS501G, Microprobe Inc), were implanted in
 147 the medullary pyramidal tract (PT) ipsilateral to the recorded M1, using a double angle stereotaxic
 148 technique, with initial targets A0 ML0.7 DV-6 relative to interaural line. During electrode placement,
 149 antidromic volleys were recorded from epidural electrodes placed over M1.

150 All procedures were performed using aseptic technique under general anesthesia comprising 3–5%
 151 inhaled sevoflurane in 100% O₂, supplemented with a continuous intravenous infusion of alfentanil
 152 (25 µg kg⁻¹ h⁻¹). Post-operative care included broad spectrum antibiotic cover (coamoxyclav 140/35
 153 (Synulox): clavulanic acid 1.75 mg kg⁻¹, amoxycillin 7 mg kg⁻¹, Pfizer; cefalexin (Ceporex) 10 mg kg⁻¹,
 154 Schering-Plough Animal Health; amoxycillin (Clamoxyl LA) 15 mg kg⁻¹, Pfizer) and analgesics
 155 (buprenorphine (Vetergesic) 10 mg kg⁻¹, Reckitt and Colman Products; carprofen (Rimadyl) 5 mg
 156 kg⁻¹, Pfizer).

157 **Behavioral, neural and muscle recordings**

158 During performance of the task, the angular position of the lever was recorded (500 Hz sampling
 159 rate) concurrently with the other neurophysiological signals described below. Various task and
 160 behavioral events (such as the trial, hold and move onset) were also captured.

161 Extracellular activity was recorded from multiple neurons from the contralateral primary motor
 162 cortex (M1) and the ipsilateral SC (SC), relative to the hand carrying out the task. From M1
 163 recordings were made using a 16 channel Eckhorn drive system whilst from the SC a 5 channel mini
 164 matrix drive was used, loaded with tetrodes (all Thomas Recording, Giessen, Germany).

165 Cortical recordings targeted the hand representation of M1. Intracortical microstimulation (trains of
 166 13 biphasic pulses, 0.2ms per phase, 3ms ISI, inter-train interval of ~1s, stimulation intensity <40 μ A)
 167 was typically carried out at the start and end of each penetration to verify this.

168 Spinal recordings targeted segments C7 to T1, ipsilateral to the moving finger. Estimation of the
 169 depth of the electrodes relative to the surface of the dura for spinal recordings is prone to errors
 170 due to the progressive thickening of the dura and overlying tissues over successive days. To
 171 accommodate for this, for each spinal penetration, the depth of the first cellular activity was noted
 172 which would likely correspond to the dorsal horn. The depth of ensuing cell recordings for that
 173 session was expressed relative to this. As with M1 recordings, microstimulation (intensity up to
 174 50 μ A) was carried at the end of each recording session and by observing evoked movements and/or
 175 muscle activity we could verify that we were recording from the appropriate cervical segments and
 176 regions.

177 Waveform signals were filtered and stored (0.3-10kHz bandpass filter, gain 2-10k, sampling rate
 178 25kHz) for offline analysis in conjunction with the behavioral task signals. Local field potentials were
 179 also recorded from the same electrodes (3 – 100Hz bandpass filtered, 1k- 5k gain, 500 Hz sampling
 180 rate).

181 Electromyographic (EMG) recordings were available from subcutaneous patch electrodes implanted
 182 over the following muscles: flexor digitorum superficialis (FDS), flexor digitorum profundus (FDP),
 183 flexor carpi radialis (FCR), flexor carpi ulnaris (FCU), extensor carpi ulnaris (ECU), extensor digitorum
 184 communis (EDC), extensor carpi radialis (ECR), abductor pollicis longus (AbPL), first dorsal
 185 interosseus (1DI), abductor pollicis brevis (AbPB, Monkey D only). As AbPB and AbPL had very weak
 186 and infrequent responses to the perturbation and they did not control the digit being perturbed,
 187 their responses will not be considered further in the paper. EMG signals were sampled at 5 kHz (gain
 188 0.5–2 K, 30 Hz to 2 kHz bandpass). Before any analysis, raw EMG signals had any DC offset removed
 189 and were then full wave rectified.

190 Neurons in M1 were identified as corticospinal if they responded to single pulse stimulation of the
 191 PT (stimulus intensity < 400 μ A, bi-phasic pulse, 0.2ms duration per phase, repetition rate ~1Hz) with

192 a constant ($<0.1\text{ms}$ jitter) antidromic latency and if they showed a constant collision interval (as in
193 Lemon 1984).

194

195

196 **Testing of peripheral inputs**

197 For the spinal recordings, some of the neural responses to peripheral stimulation were tested, either
198 before or after the recording session. This was carried out by manipulating the surface of the skin,
199 muscles, and joints of the fingers, wrist and arm to establish the receptive field of the unit. In many
200 cases it was possible to distinguish between cutaneous and deep modalities, and the presence or
201 absence of a receptive field could be readily confirmed.

202 **Analysis**

203 The response of neurons to a particular event or stimulus was analyzed by compiling peri-event time
204 histograms (PETH), whereby neural activity was aligned to the event of interest, binned (non-
205 overlapping bins, width = 1 ms, unless otherwise stated), and averaged across trials. This was then
206 smoothed by convolving with a Gaussian kernel (unit area, width parameter $\sigma=2\text{ms}$), which then
207 allowed measurement of response latency and amplitude relative to the event of interest.

208 Lever velocity and acceleration were estimated by differentiating the lever position signal once and
209 twice respectively. The time of peak velocity was used initially to align neural and muscle activity
210 across trials. The estimated mean onset latency of the perturbation for a given recording session was
211 then taken as the time point at which the lever acceleration exceeded 2 standard deviations from
212 baseline.

213 The activity of muscles and many cells was not always stationary around the time of the
214 perturbation and this could make estimating onset latency and response amplitude problematic. To
215 compensate for this, a regression line was fitted to a 100ms epoch prior to the perturbation. This
216 line was then extrapolated to 100ms after perturbation onset and subtracted from the response.

217 The onset latency of EMG and cell responses to the perturbation was then estimated by taking the
218 first instance within the first 75ms post-stimulus where all values were larger or smaller than the
219 adjusted baseline for at least 5ms. The mean value within this 5ms epoch was then compared (t-
220 test, $p<0.005$) with the distribution of mean values of 200 randomly selected epochs of the same
221 width from the pre-stimulus region.

Cells in both M1 and SC with direct connections onto motoneurons (cortico-motoneuronal cells; CM or spinal premotor cells; PM) were identified through spike triggered averaging of EMG for each muscle recorded from. Significant post-spike effects were detected as described in Williams et al. (2010). To avoid spurious effects in these averages caused by the fact that both cells and muscles responded to the perturbation, spikes that occurred 0-100ms after the perturbation were excluded when compiling the averages.

Response ratio between areas

It was of interest to compare the fraction of cells that were active at various delays post-perturbation. For each cell, after the subtraction of baseline activity from the PETH (as described above), the SD was estimated from the 100ms pre-perturbation epoch and any bins that were larger or smaller than the 95% confidence limits were considered as significantly modulated. This was then used to create an estimate of what fraction across a population of cells was active at any given time point post-perturbation.

It was also of interest to examine how the ratio of responsive cells active between the two recorded areas evolved over time, as that could give an indication of whether one group of cells was more or less involved than the other at a given epoch. This was simply estimated by

$$RespR(t) = SC(t)/M1(t) \quad \text{Eq. (1)}$$

Whereby SC (t) is the fraction of responsive cells in the spinal cord at time t that are significantly different from baseline - M1(t) is the same but for M1. Values >1 indicate that a higher fraction of spinal cells were active compared to M1 at a given time, and the inverse is true for values <1. In order to detect whether the *RespR* was significantly different from 1, a shuffling approach was taken whereby the identity of cells (SC vs M1) was randomly shuffled 500 times, before the same calculation was carried out. If the *RespR* value of the real data was outside the 95% confidence limits of the shuffled data then the ratio was considered significantly different from 1.

Modulation of cell activity with the task

The activity of M1 cells during the task has been discussed in previous work (Soteropoulos et al. 2012; Williams et al. 2009). For the present study it was of interest to examine whether cells responded differentially for flexion vs extension trials, as that would indicate activity specific to task performance rather than a general response to movement (e.g. postural stabilization). To do this PETHs were generated aligned to the end of the successful flexion and extension trials separately, and smoothed with a Gaussian kernel (width parameter $\sigma=2\text{ms}$). From these PETHs we calculated the directionality index (DI) as follows:

$$DI(t) = |(flex(t) - ext(t))/max(flex, ext)| \quad \text{Eq. (2)}$$

Whereby the directionality index (*DI*) at time *t* was the absolute difference between the firing rate during flexion (*flex*) and extension (*ext*) trials at time *t*, divided by the maximal rate seen during either trial. A *DI* value of zero indicates an identical rate during extension and flexion trials; values close to one indicate a substantial difference between the two trial types. For each cell the mean values of the *DI* during the three task phases (first hold, ramp, second hold) were averaged to generate a mean *DI* for that neuron. To detect whether this was significantly different from zero, 200 shuffled PETHs for flexion and extension trials were generated where the identity of the trial was randomized and the mean *DI* was recalculated for each shuffle. If the *DI* value of the real data was greater than 10 of the *DI* values from shuffled data then the *DI* was considered significantly different from zero ($P < 0.05$).

Estimates of peripheral and central delays

In order to estimate the potential contribution of neural activity in M1 and SC to responses in muscles an estimate of the peripheral conduction delays was required. To obtain this we estimated the latency of the muscle responses to PT stimulation, which was typically carried out during the M1 recording sessions to test for PTN cells. From each onset latency we subtracted 1.7ms, comprising the conduction delay from the PT electrode to the SC (typically ~0.6ms), a 1 ms synaptic delay from corticospinal axons to motoneurons and an additional 0.1ms utilization time to allow for the PT stimulus to activate PT axons. This latency is an estimate of the *fastest* efferent delay from SC to muscle. To estimate the afferent delay from muscle to cord, we needed to scale the calculated efferent delay by the ratio of the conduction velocities of Group Ia afferents (~85m/s, Cheney and Preston 1976) and motor efferents (~75m/s (Eccles et al. 1968)). The sum of the efferent and afferent delays plus 1ms for synaptic transmission allowed us to estimate the *fastest* possible latency for the monosynaptic stretch reflex for each muscle, excluding the mechanical delay for spindle activation.

278

Results

A total of 211 neurons were recorded from M1 (monkey D:102, monkey R:109), from 66 penetrations (39 in D, 27 in R). Sixty M1 cells were identified as PTNs (30 in D, 30 in R) and an additional 19 as CM cells (6 in D, 13 in R). Unidentified neurons (UIDs) were recorded from the same penetrations and locations as PTN/CM cells and were thus likely also to be layer V pyramidal cells. From the SC, 42 penetrations (18 in D, 24 in R) yielded 119 neurons, (24 in D and 95 in R), with 26 of those identified as PM cells (3 in D, 23 in R). The yield of CM/PM cells is comparable to yields from

286 previous studies (e.g.(Takei and Seki 2010)) as identification of such cells necessarily only happens
287 after the data is collected.

288 **Muscle responses to mechanical perturbation**

289 The rapid return of the lever produced peak lever velocities often in excess of $200^{\circ}/s$. For >88% of
290 recording sessions in both M1 and SC, the mean peak velocity across all trials was $> 200^{\circ}/s$ (range of
291 mean peak values: $115 - 442^{\circ}/s$). Figure 2A shows the lever position signals for a typical recording
292 session in gray, aligned to peak velocity. The gray shaded area is expanded in Fig. 2B which now
293 shows the velocity traces of the lever; for this session many trials had a peak velocity in excess of
294 $200^{\circ}/s$. Figure 2C shows the lever acceleration. The perturbation was sufficient to produce a robust
295 response in this session from all recorded muscles (Fig. 2D).

296 The response incidence for each muscle is shown in Fig. 3A; Fig. 3B illustrates the number of muscles
297 responding in a session. Almost all (98.6%) sessions showed a response in at least one recorded
298 muscle, whilst most sessions (80%) showed a response in at least two of the intrinsic hand and
299 forearm flexor muscles (1DI, FDS, FCU, FCR or FDP). Figure 3CDE shows the temporal profile of the
300 response for the different muscles across sessions; at each time point is plotted the fraction of all
301 sessions with EMG larger than $2 \times SD$ of the background epoch. For all muscles recorded the response
302 to the perturbation continued for more than 70ms after the perturbation.

303 In order to determine the possible contributions of neural activity to muscle responses we needed
304 an estimate of peripheral conduction time. Figure 4 shows exemplar EMG responses to PT
305 stimulation that were used to estimate the efferent delay from motoneuron to muscle (see
306 Methods). Figure 5A shows the mean response for different muscles, aligned to the onset of the
307 perturbation. EMG responses are scaled as a percentage of the 100ms period before the
308 perturbation. Under each muscle trace is the estimated peripheral loop time for each muscle
309 (triangle, black for monkey D and gray for monkey R). Dots show response latencies for that muscle,
310 measured from single sessions in each animal. The peripheral delay estimates were typically
311 consistent to within 1.3ms between the two monkeys. The exception to this was the 1DI muscle, for
312 which monkey R had an estimated loop time of 12.4 ms compared to 15.5ms for monkey D. Monkey
313 D was the larger of the two (8 vs 5.2 kg); this difference may in part represent the extra conduction
314 delay associated with longer arms. An additional contribution to the difference between animals
315 could come from differences in the implantation location of the recording wires relative to the
316 motor point within the muscle. For forearm muscles, peripheral loop times were 7 to 10.3 ms. Figure
317 5B shows a histogram of the response latency after the perturbation for each muscle, aligned

relative to the respective peripheral loop time. The bottom histogram shows a combined histogram for all muscle responses.

These analyses show that the various muscles controlling the index finger were robustly activated from the perturbation with onset delays consistent with activation of fast afferents.

Neural responses to mechanical perturbation

In both M1 and SC a substantial (>50%) fraction of neurons showed a significant response to the perturbation. Figure 6 shows the PETH and raster plots of three SC neurons, with their activity aligned to the onset of the perturbation. Across all cells, a minimum of 18 perturbations were used to generate the PETHs (mean 481, range 18 to 1102).

The frequency of responses to the perturbation is shown as pie charts for unidentified cells in the SC in Fig. 7A. The frequencies for premotor interneurons identified through spike triggered averaging of the activity of eight muscles are shown Fig. 7B. Most of the spinal PM cells (23/26) showed post-spike facilitation. More than half of all spinal neurons (56%) showed a significant response to the perturbation, and of those, 67% showed an increase in firing rate as the earliest component of their response (red pie chart sections). To the right of the pie charts are rasters representing the responses of individual cells. Bins are colored red if $> 2 \times \text{SD}$ of the baseline, and blue if $< -2 \times \text{SD}$. Figure 7C shows the mean responses of cells to the perturbation, with the baseline subtracted as discussed in the METHODS section. Red, blue and black lines show averages for cells with a significant increase, decrease or no change in firing after to the perturbation (positive, negative or unmodulated cells). There was no significant difference (one way ANOVA, $F=0.44$, $p=0.64$) in the baseline activity between positive, negative and unmodulated cells (mean baseline values of 24.6, 28.9 and 23.6Hz respectively). Positive cells had a significantly ($p<0.001$, un-paired t-test) larger response amplitude (mean 21 Hz above baseline) compared to negative cells (mean 7.1 Hz below baseline). However, as response amplitude is expressed relative to baseline then there is a flooring bias for negative cells (firing rate cannot go lower than zero).

Figure 7D is a histogram of the depth that cells were recorded from, with gray showing all cells and black identified PM cells. The line in red corresponds to the fraction of cells at a given depth that responded to the perturbation. There was a significant correlation (Pearson's correlation, $R^2 = 0.76$, $p<0.0003$) between incidence of response and depth of recording. Although we cannot definitely identify the laminar location of our neural recordings, cells recorded from the more superficial depths had a much higher incidence of response compared to deeper recordings, which is consistent

349 with the known termination pattern of sensory afferents in the SC (Edgley and Jankowska 1988;
350 Molander and Grant 1985; Riddell and Hadian 2000; Woolf and Fitzgerald 1986)

351 For some of the spinal cells ($n=95$) we were able to test responses to peripheral stimulation and
352 found that a majority (73%) was responsive. Of the PM cells that were tested ($n=18$) the fraction
353 responding to peripheral stimulation was 61% ($n=11$). Figure 7E shows the depth distribution of cells
354 with cutaneous (black) and deep (gray) receptive fields. At depths that would correspond to
355 superficial layers of the SC ($<0.5\text{mm}$), most (85%) of the tested SC cells responded to peripheral
356 stimulation and of those, most responded to cutaneous stimulation (69%). Figure 7F is focused on
357 cells responding to cutaneous inputs from the hand (black line), and a similar pattern as Fig. 7E is
358 seen. Of the 25 cells with responses to cutaneous stimulation in the hand, most ($n=21$, 84%) also
359 responded to the finger perturbation (red line).

360 Figure 8 is a comparable figure but for the M1 cells. More than two thirds of all M1 cells (70%)
361 showed a significant response to the perturbation, and of those, 59% showed an increase in firing
362 rate as the earliest component of their response. Figure 8A shows a pie chart of the fraction of M1
363 unidentified cells responding to the perturbation, and a raster indicating the response timing. Similar
364 plots for PTNs and CM cells are shown in Fig. 8BC. Figure 8D shows the mean responses of cells to
365 the perturbation. Unlike for spinal cells, there was a significant difference between the baseline
366 firing rate of positive (mean 14.9Hz), negative (19.6Hz) and unmodulated (10.8Hz) cells (one way
367 ANOVA, $F=8.59$, $p=0.0003$). As with spinal cells, positive cells had a significantly ($p<0.001$, un-paired
368 t-test) larger response amplitude (8.8Hz) compared to negative cells (5.1Hz), although the same
369 flooring caveat applies as described previously for SC cells.

370 Figure 9 compares the firing responses of cells between M1 and SC. Figure 9A and B show boxplots
371 of baseline firing rates for the different cell types (Fig 9A is for cells without a significant response to
372 the perturbation and Fig. 9B is for responsive cells). Spinal neurons had significantly higher firing
373 rates than cells in M1 (25Hz vs 15.1 respectively, unpaired t-test, $p<0.0001$). A one way ANOVA of
374 baseline firing vs cell type for cells with a significant response to perturbation was significant
375 ($F=4.05$, $p=0.0035$) and a post-hoc analysis revealed that both spinal unidentified and PM cells had
376 higher rates compared to M1 unidentified cells, but not PTNs or CM cells (Tukey-Kramer, adjusted
377 for multiple comparisons, $p<0.05$). A comparison of cells without any significant response to
378 perturbations produced the same results (M1 vs SC, t-test, $p<0.0001$).

379 Figure 9C shows the magnitude of the responses (relative to baseline) for each cell type. For the
380 purposes of this plot, the absolute value of response was used, such that cells with rate suppressions
381 contribute positive values to the population. As with baseline firing, spinal neurons had a

significantly higher response magnitude compared to M1 cells (10.2Hz vs 5.2Hz respectively, unpaired t-test, $p < 0.0003$). A one way ANOVA of response magnitude vs cell type was significant ($F = 9.1$, $p < 8 \times 10^{-7}$). Post-hoc analysis revealed that spinal unidentified cells had significantly higher response magnitudes compared to all other cell types (Tukey-Kramer, adjusted for multiple comparisons, $p < 0.05$).

To characterize how detectable a response to perturbation would be against baseline firing, we examined the ratio of the response relative to the background firing rate (signal to baseline ratio, SBR; Soteropoulos and Baker 2007; Soteropoulos et al. 2012). This is useful, as the same response magnitude would clearly be easier to detect in a cell with low compared to a high firing rate. The values of SBR are shown in Fig. 9D. There was no significant difference either between areas (all SC cells vs all M1 cells, $SBR = 0.87$ vs 0.89 respectively, unpaired t-test, $p > 0.1$) or between different cell types (one way ANOVA, $F = 1.01$, $p = 0.4$). This suggests that, relative to their background firing activity, cells in the SC responded to the perturbations just as robustly as cells in M1.

Latency of responses to perturbation

The latency of the onset of neuronal responses to the perturbation is shown in Figure 10 for cortical and spinal cells. Figure 10A shows the cumulative distribution of response latency from all M1 (black line) and SC (gray) cells. There was significant difference between M1 and SC in terms of mean latency (unpaired t-test, $p < 0.017$; mean latencies 21.7 ms vs 25.5 ms for SC and M1 respectively). There was substantial overlap in latencies between the cells from the two areas, although the SC had many more latencies < 10 ms than M1 (13% vs $< 1\%$ of cells respectively, left of dotted line, Fig. 10A).

The colored histograms in Fig 10B show the latency distributions for the different cell types (mean latency M1 unidentified: 27 ms, PTNs: 23.3 ms, CM cells: 24 ms, SC unidentified: 20.4 ms, PM cells: 26.3 ms). A one way ANOVA comparing response latency with cell type was significant ($F = 3.41$, $p = 0.009$), and post-hoc analysis revealed that the most significant difference was between the unidentified cells in M1 and the SC (Tukey-Kramer, adjusted for multiple comparisons, $p < 0.05$).

There was no significant difference in onset latency between SC cells that responded to cutaneous stimulation in the hand and those with responses to other types of stimulation or without sensory responses (one way ANOVA, $F = 0.67$, $P > 0.5$).

Contribution of spinal premotor and corticomotoneuronal cells to EMG responses.

Due to concurrent recordings of EMG with neural activity, we were able to identify some cells as being pre-synaptic to motoneurons using spike-triggered averaging (see Methods). As some of these cells also responded to the perturbation, they could have contributed to muscle responses (Cheney

414 and Fetz 1984). An exemplar premotor spinal cell is shown in Fig. 11. Figure 11A shows the raw
 415 recordings for 10 perturbations, and underneath is the mean EMG for those 10 perturbations from
 416 the muscle the cell was presynaptic to; in this case it was the 1DI muscle. Figure 11B shows the mean
 417 response of the same premotor cell and muscle across all perturbations indicating the earlier onset
 418 of the neural response compared to that of the muscle.

419 Although every action potential of CM and spinal PM cells generated a postsynaptic response in its
 420 target motoneurons, if the response of a cell to the perturbation occurred well after the EMG
 421 response, then a contribution would be far less likely than if the cell responded before or during the
 422 EMG response. In order to examine the cell response timing in this framework, we first estimated
 423 the reflex loop time for each cell (Fig 12A). This was calculated to estimate the time it takes for the
 424 peripheral stimulus to reach the motoneurons, via the cell of interest.

425 To calculate the loop time for a given cell, we simply summed the delay with which the cell was
 426 activated following a perturbation (Fig. 12B, $t_{sensory}$) with the delay estimated from spike-triggered
 427 averaging between the cell and its target muscle (Fig. 12C, t_{motor}). For the example cell shown in Fig.
 428 11 these values are 26.5ms and 9.1ms respectively, giving a total of 35.6ms total loop time. By
 429 measuring the offset and onset of the EMG response to the perturbation (Fig 12D), the loop time
 430 could then be used to determine whether the cell could contribute to the EMG activation. For this
 431 example cell, the loop time was within the response period in the muscle, indicating that the cell
 432 could contribute to the EMG response.

433 Figure 13 shows the results of this analysis carried out for the CM/spinal PM cells that responded to
 434 the perturbation and whose target muscles also had clear responses. Note that the same cell could
 435 contribute to more than one loop time estimate if it was presynaptic to multiple muscles, which in
 436 turn responded to the perturbation. Figure 13A shows the duration of the EMG response (gray
 437 squares) for the particular muscle that the premotor cells were presynaptic to and the colored
 438 markers show the loop delay. Red markers are for CM cells ($n=15$) and cyan markers are for spinal
 439 PM cells ($n=11$). Traces have been sorted in order of EMG onset latency.

440 All but two cells (both PM) have loop times before or during the EMG response period, consistent
 441 with a contribution to the EMG response. Figure 13B1 shows the mean EMG response across all
 442 effects shown in Fig. 13A. Figure 13B2 shows the distribution of loop times.

443 The loop delay of all premotor effects was between 10 and 50ms after the perturbation, and this
 444 was within 15ms of the EMG onset for most effects (68%). In 30% of cases the cell response began
 445 before the onset of EMG. Most EMG responses were long lasting (range 22 to 86ms), which is well

beyond the width of most motor units recorded from the muscle surface by spike-triggered averaging from an intramuscular-recorded single unit (typically <25ms; Baker and Lemon 1998; Lemon et al. 1990). This implies that the EMG response was composed of motor units firing at a range of delays. Premotor cells whose contribution would reach the muscle after the onset of the EMG response could contribute to the activity of motor units activated later on in the response.

The data were replotted in Fig. 13C, as a histogram of neural loop time relative to EMG onset latency. In addition we also show the fraction of the cases where EMG activity continued at a given time after the onset. All EMG recordings showed continued activity for at least 22 ms after the response onset; by this time, a large fraction of responding premotor cells in both M1 (84%) and SC (66%) had loop times consistent with contributing to the response.

To summarize, these results show that the response onset of cells that are presynaptic to MNs, both in M1 and SC, occurs at delays that would allow most of the cells to contribute to the ongoing EMG response.

Relative Contributions of M1 and SC to EMG responses.

Analysis from the previous section showed that premotor cell responses from both M1 and SC occurred at latencies consistent with a contribution to the EMG responses. It is then of interest to examine the relative contribution of M1 and SC to the EMG response. It might be expected that SC cells would mostly contribute to the earlier components of the EMG response and M1 cells to the later components.

To investigate the relative contributions of M1 and SC to responses, we compared the fraction of cells from each area that was significantly different from baseline at various delays after the perturbation onset. The results from this analysis are shown in Fig. 14. Figure 14A shows the fraction of responsive cells in each area that are active post-perturbation. Figure 13B shows the ratio of the response fraction between the two areas (*RespR*, Eq. 2 in Methods). The dotted lines show the 95% confidence limits on the ratio calculated from shuffled data. Although the ratio is > 1 during the early parts of the response and <1 later on, it does not cross the confidence limits, suggesting that M1 and SC make similar contributions during the first 100 ms of the response to the perturbation.

Simply comparing the responses of M1 and SC cells relative to perturbation onset does not take into account the added conduction delay from M1 to muscles. We could shift all M1 responses by ~ 1.2ms to account for this, as that would be the fastest delay from M1 to motoneurons in the cervical enlargement. However, our dataset included identified PTNs. As part of the identification process, we measured the antidromic latency following pyramidal tract stimulation in the medulla, and

478 subtracted 0.1ms as utilization time). Since the pyramidal electrodes are approximately half way
 479 between M1 and the cervical enlargement, this enabled us to calculate an accurate estimate for the
 480 delay from M1 to SC for each cell individually, simply by doubling the measured antidromic latency.
 481 The results of this analysis are shown in Fig 14CD; the abscissa now shows time relative to the
 482 perturbation, measured when responses reach the SC. Early after the perturbation (11-21 ms) the
 483 *RespR* was significantly greater than one (mean 3.3), indicating that 3.3 times more SC cells than M1
 484 cells contributed to the EMG response. Later on (35-41ms), the *RespR* was significantly smaller than
 485 one, suggesting that 1.3 times more M1 cells than SC cells contributed during this period. There
 486 were two further, brief, crossings of the confidence limits 80-90 ms after the perturbation (triangles,
 487 Fig. 14D); other than these epochs, there was no significant difference in the *RespR* during the rest
 488 of the 100 ms period after the perturbation.

489 In the same way that recordings in the cortex from unidentified cells are likely to be biased towards
 490 the larger pyramidal neurons, it is also possible that a similar bias exists in our spinal recordings from
 491 unidentified neurons. This might include ascending projection neurons, such as spinocerebellar cells,
 492 that would probably have larger extracellular spikes. To exclude this possibility we repeated the
 493 analysis in Fig 14AB but we only used identified premotor cells from the SC compared to M1 PTNs
 494 and the results are shown in Figure 14CD. As before, early after the perturbation (14-17ms)
 495 premotor SC neurons have a significantly higher *RespR* value than M1 PTNS (mean of 4.7). A higher
 496 fraction of M1 PTNs is active later on (35-41ms: mean 1.4, 88-93ms: mean 1.9). Figure 14E shows, for
 497 comparison, the fraction of muscle recordings with activity significantly different from baseline.
 498 Results are shown by different lines for distal (1DI), forearm flexor (Flx) and extensor (Ext) muscles.
 499 The curves for each muscle have been adjusted by correcting by the respective efferent conduction
 500 delay; this means that all latencies are shown relative to activity in the SC, providing a consistent
 501 time frame for comparison with Fig. 14CD. The triangles show the actual time of perturbation for the
 502 different EMG traces.

503 To summarize, the very earliest part of the EMG response is dominated by the SC. There are brief
 504 (<7 ms) periods in the later part of the response with a slightly greater contribution of M1 than SC,
 505 but for most of the EMG response period M1 and SC seem to make similar contributions.

506

507 **Do Spinal Cells Respond Directly to the Perturbation, or Indirectly to M1 Activation?**

508 Many SC interneurons are also known to receive descending inputs from the cortex (Jankowska et al.
 509 1976; Lundberg and Voorhoeve 1961; Riddle and Baker 2010) and indeed PT terminations are

510 densest in the intermediate layers of the SC in the monkey (Dum and Strick 1996). It is thus possible
511 that for some spinal cells, the response after a perturbation is produced by descending activation
512 from M1 instead of directly from afferent stimulation. We cannot directly address this, but we can
513 exploit our knowledge of the antidromic latency of the PTNs to determine what fraction of SC cell
514 responses were too early to have been initiated due to M1 activity. To do this, PTN responses to the
515 perturbations were again adjusted by adding twice the antidromic latency to account for the
516 conduction delay from the cortex to the spinal cord. An additional 1 ms was added to account for
517 the synaptic delay between corticospinal fibers and SC cells.

518 The results of this analysis are shown in Figure 15. Figure 15A shows the cumulative distribution of
519 SC (cyan) and adjusted PTN (red) response latency. The mean adjusted PTN response latency was
520 27.8ms (range 13 – 64.2ms). The two distributions were significantly different (two-sample
521 Kolmogorov-Smirnov test, $p < 0.001$, KS statistic=0.44). 23% of SC cells had onset latencies that were
522 shorter than the earliest PTN adjusted latency, which appeared to be an anomalous single
523 measurement. Excluding that single PTN, 46% of SC cells had an earlier onset latency than the PTNs.
524 This fraction is 38% if we only consider spinal PM cells. This relationship was examined further by a
525 percentile plot (Fig. 15B). This shows the percentage of SC cells with latencies too early to be
526 mediated by a given percentage of PTN cells (thick black line). This is clearly above the identify line
527 (dotted), indicating that the SC cell population consistently responded earlier than PTNs.

528 In primates there are relatively few corticospinal terminations from M1 in the most dorsal layers of
529 the SC (Dum and Strick 1996; Yoshino-Saito et al. 2010). If we assume that the most superficial SC
530 cells (recorded < 0.5 mm from the first cells encountered in the penetration) could not have
531 responses mediated through M1, we can adjust the percentile plot accordingly. This amended plot is
532 shown as the thin line in Fig. 15B. The overall fraction of SC cells that could not have their responses
533 initiated through any M1 PTN becomes $> 49\%$ (rising to $> 63\%$ if we exclude the earliest, potentially
534 anomalous PTN response). These estimates should be considered conservative as they assume a
535 monosynaptic connection; in reality, some effects from the corticospinal tract to SC cells will take a
536 more indirect route which would require a larger compensation than the 1 ms synaptic delay which
537 we allowed. Additionally, our dataset of PTN recordings is biased towards the fastest PTNs (Firmin et
538 al. 2014; Innocenti et al. 2019; Kraskov et al. 2018; Kraskov et al. 2019). If M1 contributes to SC
539 responses through the many PTNs which are even slower than those recorded here, then M1
540 contributions to SC responses would be even smaller than assessed here.

541 We conclude that a substantial fraction of SC responses to the perturbation were too early to be
 542 initiated by descending activation from PTNs. However, our results do not preclude a contribution to
 543 the latter components of the SC response, or to SC cells with late responses.

544 **Directionality Index.**

545 The results so far have shown that cells in both M1 and SC respond to mechanical perturbation, but
 546 if the cells that respond to the perturbation have minimal activity during the task, then that would
 547 limit the functional relevance of our results. To address this we examined how active cells were
 548 during the task, and in particular whether cells were differentially active during flexion vs extensions
 549 trials by calculating a Directionality Index (DI, see Methods). Cells that show a large modulation in
 550 firing during the task, but whose response was similar across flexion and extension trials, would
 551 result in a low DI value. These could be of lesser interest, as their activity could be postural and less
 552 directly related to task performance. The results of this analysis are shown in Figure 16.

553 The top trace in Fig. 16A and B shows the PETH of two SC cells for flexion (blue) and extension (red)
 554 trials, and the lower trace shows how the DI index modulates during the trial. The first cell (Fig 16A)
 555 was very active during the ramp and second hold part of flexion trials, but inactive in these phases
 556 during extension trials. This resulted in a high DI (0.7). For the second cell (Fig. 156) although it had a
 557 very high firing rate overall and a clear response to the perturbation, the activity during the two
 558 movements was very similar (DI=0.07). The vertical dotted lines in Fig. 16AB demarcate the
 559 movement phases of the task (Hold 1, Ramp, Hold 2), and Fig. 15C shows the average lever angle
 560 signals for flexion (blue) and extension (red) trials.

561 Figure 16D shows the distribution of DI values for all M1 cells (black bars) and all SC cells (grey).
 562 There was no significant difference between the two areas (mean DI for M1: 0.42, for SC: 0.41,
 563 $p>0.1$, unpaired t-test). Most cells (>87%) in both areas had a DI value significantly different from
 564 zero, but there was no difference between cells with and without a response to the perturbation
 565 (Fig. 16E, one way ANOVA, $F=0.44$, $p>0.7$). The same conclusions hold if we only consider spinal PM
 566 cells that do (mean DI=0.45) and don't (mean DI=0.44) respond to a perturbation (unpaired t-test,
 567 $p>0.8$). We conclude that most cells in our dataset were differentially active in flexion vs extension
 568 trials, including those that responded to the perturbation.

569

570 **Discussion**

571 The neural origin of later components of the stretch reflex remains under debate. Whilst a
 572 supraspinal contribution is well supported, our results affirm that the SC is also likely to play a role.
 573 SC cells, including premotor interneurons, responded as robustly as M1 neurons to a mechanical
 574 perturbation of the index finger, at latencies compatible with contributing to the EMG response.
 575 The response of SC neurons to mechanical perturbations has been rarely studied in the upper limb
 576 (Fetz et al. 2002) and to the best of our knowledge this is the first time that SC neurons, including
 577 premotor interneurons, have been shown to respond to a mechanical perturbation in the fingers in
 578 the awake behaving primate. Below we consider some implications of this finding.

579 We should be cautious in assigning the spinal responses as arising from a single source. Many spinal
 580 neurons receive both afferent and descending inputs (Fig 1), and these could both potentially
 581 contribute to spinal activity at different delays after the perturbation. For at least some of the spinal
 582 cells it is highly likely that the initial response mediated through sensory afferents was too rapid to
 583 be mediated through supraspinal pathways (Fig 15). The rapid lever motion of our paradigm should
 584 be highly effective in activating Group Ia afferents, but other proprioceptive fibers (e.g. Group Ib and
 585 II) most likely also responded as during natural movements all three types can respond to rapid
 586 changes in muscle length (Dimitriou and Edin 2008a; b), most likely due to fusimotor drive.
 587 Cutaneous afferents are also likely to contribute to some of the responses - indeed, most SC cells
 588 responding to cutaneous stimulation in the hand responded to the perturbation as well (Fig. 7F) and
 589 these cells were more superficially located, matching the known termination patterns of cutaneous
 590 afferents in the dorsal SC (Edgley and Jankowska 1988; Maxwell et al. 2000; Molander and Grant
 591 1985; Woolf and Fitzgerald 1986).

592 A further contribution to the activation of spinal neurons could be made via descending pathways,
 593 originating from the cerebral cortex and brainstem (Lemon 2008). These pathways project to
 594 motoneurons as well as to interneurons in the intermediate spinal laminae (Alstermark and Isa 2012;
 595 Lundberg 1979a). As these systems can also respond to perturbations (Herter et al. 2015;
 596 Soteropoulos et al. 2012), supraspinal corrective responses could thus reach motoneurons not just
 597 directly but also filtered through spinal interneurons. Descending contributions would require an
 598 extra delay for the sensory signal to reach the cortex or brainstem and the response to come back
 599 down to the spinal cord. The SC therefore probably contributes to muscle responses for far longer
 600 than typically considered but should be best characterized as a mix of afferent and descending
 601 sources. Some human studies have also indicated a spinal contribution to the LLR (Lewis et al. 2004;
 602 Lourenco et al. 2006).

603 **Implications for motor control**

604 A key feature of the LLR is its behavioral flexibility: the reflex amplitude can modulate according to
 605 the requirements of a manual task (Hammond 1956; Pruszynski et al. 2008; Yang et al. 2011).
 606 Supraspinal areas are usually thought to subserve this, because they not only respond to mechanical
 607 perturbations with permissive latencies, but are also highly active during task performance. In the
 608 cortex M1 is well established to be a critical area for voluntary movements, particularly involving the
 609 distal forelimb, and many studies show that cells in M1 modulate their activity during action.
 610 Further down the neuraxis, the engagement of the red nucleus during voluntary reaching and
 611 grasping movements has been known for some time (Alstermark and Isa 2012; Cheney 1980; Gibson
 612 et al. 1985a; b; Otero 1976), although the near-absence of a rubrospinal tract in man (Nathan and
 613 Smith 1982) makes rubrospinal contributions to the LLR unlikely in humans. The brainstem RF, once
 614 thought to contribute mostly to posture and locomotion, is now also known to be highly active
 615 during voluntary movements with the upper limb (Buford and Davidson 2004b; Schepens and Drew
 616 2006; 2004; Schepens et al. 2008), including during more isolated finger movements (Soteropoulos
 617 et al. 2012).

618 SC neurons are also active during voluntary movements. Cells in the SC can be highly active during
 619 non-movement epochs in instructed delay tasks (Prut and Fetz 1999), much like the premotor cortex
 620 (Churchland et al. 2006; Crammond and Kalaska 2000; Kalaska and Crammond 1995; Kurata and
 621 Wise 1988) and reticular formation (Buford and Davidson 2004a). Spinal interneurons are active
 622 during whole arm movements such as reaching to grasp (Riddle and Baker 2010) as well as for more
 623 isolated wrist (Shalit et al. 2012) and grasping actions (Alstermark and Isa 2012; Takei and Seki 2010;
 624 2013). Combined with the results of this study showing that SC cells respond to perturbations with
 625 permissive latencies, the SC thus fulfils the same criteria for contributions to the LLR as for M1.

626 Most experimental paradigms have examined upper limb LLR responses while subjects are seated
 627 and in a stable posture (although see (Marsden et al. 1981)). However during everyday actions,
 628 unexpected perturbations need to be accommodated not just based on what the hands are doing
 629 but also on the involvement of the rest of the body, taking into account posture and any locomotion.
 630 It is well established that spinal circuits integrate inputs from multiple descending pathways,
 631 including systems that are critical for locomotion and posture, such as the reticulo- and
 632 vestibulospinal projections (Bannatyne et al. 2009; Cabaj et al. 2006; Illert et al. 1981; Isa et al. 2006;
 633 Jankowska et al. 2005; Krutki et al. 2003; Riddle and Baker 2010; Stecina et al. 2008) As such, SC
 634 premotor circuits are optimally placed to allow the LLR to be coordinated within a much broader
 635 behavioral context, although this remains to be explicitly shown.

636 Following motor damage such as from stroke and spinal cord injury or in neurodegenerative
637 conditions such as Parkinson's Disease, a substantial fraction of patients develop hypertonia and
638 hyperreflexia (Angulo-Parker and Adkinson 2018; McGregor and Nelson 2019). Multiple systems
639 along the neuraxis are likely to contribute to this, but our results lend further support to the
640 evidence that changes in spinal circuitry could contribute to reflex gains (D'Amico et al. 2014).

641 **LLR: beyond a marker for cortical excitability?**

642 The LLR is sometimes used as a non-invasive correlate of M1 excitability even though it has become
643 clear over the last 20 years or so that its locus is far from singular (Kurtzer 2014; Pruszynski et al.
644 2011). For distal and forearm muscles contributions from M1 to the LLR are well supported, but
645 there is also evidence for subcortical involvement (Soteropoulos et al. 2012). For more proximal
646 muscles there is also evidence for both M1 and subcortical contributions (Foyssal et al. 2016; Herter
647 et al. 2015; Omrani et al. 2014) but the relative importance of M1 is unclear. Although cells in M1
648 are modulated during proximal limb perturbations (Omrani et al. 2014; Pruszynski et al. 2014), in
649 patients with aberrant bilateral corticospinal projections, bilateral LLRs are seen for distal (Matthews
650 et al. 1990) but not proximal muscles (Fellows et al. 1996).

651 If all contributors to the LLR modulate in the same way during behavior, or if only M1 activity shows
652 any task modulation, then there is little issue with using the LLR as a marker of M1 excitability.
653 However it is now well established that the state of both brainstem (Buford and Davidson 2004b;
654 Soteropoulos et al. 2012) and the spinal cord (Prut and Fetz 1999; Takei and Seki 2010; 2013;
655 Williams et al. 2010) modulates with behavior. Although it remains to be shown whether the
656 perturbation-evoked responses in subcortical regions modulate their size with behavioral context as
657 they do in M1, particularly when subjects are comfortably seated in the lab environment, caution is
658 warranted in assigning any observed task-related modulation in the LLR purely to cortical circuits.

659 **Summary**

660 Our results show that a substantial fraction of neurons in the lower cervical SC respond to a
661 mechanical perturbation of the index finger. The latency of these responses makes it highly likely
662 that the SC contributes to the muscle responses beyond the SLR, at least for the forearm and
663 intrinsic hand muscles examined here.

664

665 List of Abbreviations:

666 1DI: first dorsal interosseous

667 AbPB: abductor pollicis brevis
 668 AbPL: abductor pollicis longus (AbPL)
 669 CM: Corticomotoneuronal cell
 670 DI: Directionality index.
 671 ECR: extensor carpi radialis
 672 ECU: extensor carpi ulnaris (ECU)
 673 EDC: extensor digitorum communis
 674 EMG: Electromyographic
 675 FCR: flexor carpi radialis (FCR)
 676 FCU: flexor carpi ulnaris
 677 FDP: flexor digitorum profundus
 678 FDS: flexor digitorum superficialis
 679 LLR: Long latency response
 680 M1: Primary motor cortex.
 681 PETH: Peri-event time histogram
 682 PM: Premotoneuronal cell
 683 PT : Pyramidal tract.
 684 RespR: Spinal Cord to Motor Cortex Response Ratio
 685 RF: Feticular Formation
 686 SC: Spinal cord
 687 SLR: Short latency response
 688 UID: Unidentified cell
 689

690 **References:**

691 **Alstermark B, and Isa T.** Circuits for skilled reaching and grasping. *Annu Rev Neurosci* 35: 559-578,
 692 2012.
 693 **Angulo-Parker FJ, and Adkinson JM.** Common Etiologies of Upper Extremity Spasticity. *Hand clinics*
 694 34: 437-443, 2018.
 695 **Baker SN, and Lemon RN.** A computer simulation study of the production of post-spike facilitation in
 696 spike triggered averages of rectified EMG. *J Neurophysiol* 80: 1391-1406, 1998.

- 697 **Bannatyne BA, Liu TT, Hammar I, Stecina K, Jankowska E, and Maxwell DJ.** Excitatory and inhibitory
698 intermediate zone interneurons in pathways from feline group I and II afferents: differences in
699 axonal projections and input. *J Physiol* 587: 379-399, 2009.
- 700 **Brown AG, and Fyffe RE.** The morphology of group Ib afferent fibre collaterals in the spinal cord of
701 the cat. *J Physiol* 296: 215-226, 1979.
- 702 **Brown AG, and Fyffe REW.** The morphology of group Ia afferent fibre collaterals in the spinal cord of
703 the cat. *J Physiol* 274: 111-127, 1978.
- 704 **Buford JA, and Davidson AG.** Movement-related and preparatory activity in the reticulospinal
705 system of the monkey. *Exp Brain Res* 159: 284-300, 2004a.
- 706 **Buford JA, and Davidson AG.** Movement-related and preparatory activity in the reticulospinal
707 system of the monkey. *Exp Brain Res* 159: 284-300, 2004b.
- 708 **Cabaj A, Stecina K, and Jankowska E.** Same spinal interneurons mediate reflex actions of group Ib
709 and group II afferents and crossed reticulospinal actions. *J Neurophysiol* 95: 3911-3922, 2006.
- 710 **Cheney PD.** Response of rubromotoneuronal cells identified by spike-triggered averaging of EMG
711 activity in awake monkeys. *Neurosci Lett* 17: 137-142, 1980.
- 712 **Cheney PD, and Fetz EE.** Corticomotoneuronal cells contribute to long-latency stretch reflexes in the
713 rhesus monkey. *J Physiol* 349: 249-272, 1984.
- 714 **Cheney PD, and Preston JB.** Classification and response characteristics of muscle spindle afferents in
715 the primate. *J Neurophysiol* 39: 1-8, 1976.
- 716 **Churchland MM, Santhanam G, and Shenoy KV.** Preparatory activity in premotor and motor cortex
717 reflects the speed of the upcoming reach. *J Neurophysiol* 96: 3130-3146, 2006.
- 718 **Corden DM, Lippold OC, Buchanan K, and Norrington C.** Long-latency component of the stretch
719 reflex in human muscle is not mediated by intramuscular stretch receptors. *J Neurophysiol* 84: 184-
720 188, 2000.
- 721 **Crammond DJ, and Kalaska JF.** Prior information in motor and premotor cortex: activity during the
722 delay period and effect on pre-movement activity. *J Neurophysiol* 84: 986-1005, 2000.
- 723 **D'Amico JM, Condliffe EG, Martins KJ, Bennett DJ, and Gorassini MA.** Recovery of neuronal and
724 network excitability after spinal cord injury and implications for spasticity. *Frontiers in integrative*
725 *neuroscience* 8: 36, 2014.
- 726 **Dimitriou M, and Edin BB.** Discharges in human muscle receptor afferents during block grasping. *J*
727 *Neurosci* 28: 12632-12642, 2008a.
- 728 **Dimitriou M, and Edin BB.** Discharges in human muscle spindle afferents during a key-pressing task.
729 *J Physiol* 586: 5455-5470, 2008b.
- 730 **Dum RP, and Strick PL.** Spinal cord terminations of the medial wall motor areas in macaque
731 monkeys. *Journal Of Neuroscience* 16: 6513-6525, 1996.
- 732 **Eccles RM, Phillips CG, and Chien-Ping W.** Motor innervation, motor unit organization and afferent
733 innervation of m. extensor digitorum communis of the baboon's forearm. *J Physiol* 198: 179-192,
734 1968.
- 735 **Edgley SA, and Jankowska E.** Information processed by dorsal horn spinocerebellar tract neurones in
736 the cat. *J Physiol* 397: 81-97, 1988.
- 737 **Fellows SJ, Topper R, Schwarz M, Thilmann AF, and Noth J.** Stretch reflexes of the proximal arm in a
738 patient with mirror movements: absence of bilateral long-latency components. *Electroencephalogr*
739 *Clin Neurophysiol* 101: 79-83, 1996.
- 740 **Fetz EE, Perlmuter SI, Maier MA, Flament D, and Fortier PA.** Response patterns and postspike
741 effects of premotor neurons in cervical spinal cord of behaving monkeys. *Can J Physiol Pharmacol*
742 74: 531-546, 1996.
- 743 **Fetz EE, Perlmuter SI, Prut Y, Seki K, and Votaw S.** Roles of primate spinal interneurons in
744 preparation and execution of voluntary hand movement. *Brain Res Brain Res Rev* 40: 53-65, 2002.
- 745 **Firmin L, Field P, Maier MA, Kraskov A, Kirkwood PA, Nakajima K, Lemon RN, and Glickstein M.**
746 Axon diameters and conduction velocities in the macaque pyramidal tract. *J Neurophysiol* 112: 1229-
747 1240, 2014.

- 748 **Foysal KHMR, De Carvalho F, and Baker SN.** Spike-timing dependent plasticity in the long latency
749 stretch reflex following paired stimulation from a wearable electronic device. *Journal of*
750 *Neuroscience* 36: 10823–10830, 2016.
- 751 **Fyffe RE.** The morphology of group II muscle afferent fibre collaterals [proceedings]. *J Physiol* 296:
752 39P-40P, 1979.
- 753 **Ghez C, and Shinoda Y.** Spinal mechanisms of the functional stretch reflex. *Exp Brain Res* 32: 55-68,
754 1978.
- 755 **Gibson AR, Houk JC, and Kohlerman NJ.** Magnocellular red nucleus activity during different types of
756 limb movement in the macaque monkey. *J Physiol* 358: 527-549, 1985a.
- 757 **Gibson AR, Houk JC, and Kohlerman NJ.** Relation between red nucleus discharge and movement
758 parameters in trained macaque monkeys. *J Physiol* 358: 551-570, 1985b.
- 759 **Hammond PH.** The influence of prior instruction to the subject on an apparently involuntary neuro-
760 muscular response. *Journal of Physiology* 132: 17-18P, 1956.
- 761 **Herter TM, Takei T, Munoz DP, and Scott SH.** Neurons in red nucleus and primary motor cortex
762 exhibit similar responses to mechanical perturbations applied to the upper-limb during posture.
763 *Frontiers in integrative neuroscience* 9: 29, 2015.
- 764 **Illert M, Jankowska E, Lundberg A, and Odutola A.** Integration in descending motor pathways
765 controlling the forelimb in the cat. 7. Effects from the reticular formation on C3-C4 propriospinal
766 neurones. *Exp Brain Res* 42: 269-281, 1981.
- 767 **Innocenti GM, Caminiti R, Rouiller EM, Knott G, Dyrby TB, Descoteaux M, and Thiran JP.** Diversity
768 of Cortico-descending Projections: Histological and Diffusion MRI Characterization in the Monkey.
769 *Cereb Cortex* 29: 788-801, 2019.
- 770 **Isa T, Ohki Y, Seki K, and Alstermark B.** Properties of propriospinal neurons in the C3-C4 segments
771 mediating disynaptic pyramidal excitation to forelimb motoneurons in the macaque monkey. *J*
772 *Neurophysiol* 95: 3674-3685, 2006.
- 773 **Jack JJB, Miller S, Porter R, and Redman S.** The time course of minimal excitatory post-synaptic
774 potentials evoked in spinal motoneurons by group Ia afferent fibres. *J Physiol* 215: 353-380, 1971.
- 775 **Jankowska E, and Edgley SA.** Functional subdivision of feline spinal interneurons in reflex pathways
776 from group Ib and II muscle afferents; an update. *Eur J Neurosci* 32: 881-893, 2010.
- 777 **Jankowska E, Edgley SA, Krutki P, and Hammar I.** Functional differentiation and organization of
778 feline midlumbal commissural interneurons. *J Physiol* 565: 645-658, 2005.
- 779 **Jankowska E, and McCrea DA.** Shared reflex pathways from Ib tendon organ afferents and Ia muscle
780 spindle afferents in the cat. *J Physiol* 338: 99-111, 1983.
- 781 **Jankowska E, McCrea DA, and Mackel R.** Oligosynaptic excitation of motoneurons by impulses in
782 group Ia muscle spindle afferents in the cat. *J Physiol* 316: 411-425, 1981.
- 783 **Jankowska E, Padel Y, and Tanaka R.** Disynaptic inhibition of spinal motoneurons from the motor
784 cortex in the monkey. *J Physiol* 258: 467-487, 1976.
- 785 **Kalaska JF, and Crammond DJ.** Deciding not to GO: neuronal correlates of response selection in a
786 GO/NOGO task in primate premotor and parietal cortex. *Cereb Cortex* 5: 410-428, 1995.
- 787 **Kraskov A, Baker S, Soteropoulos D, Kirkwood P, and Lemon R.** The Corticospinal Discrepancy:
788 Where are all the Slow Pyramidal Tract Neurons? *Cereb Cortex* 2018.
- 789 **Kraskov A, Soteropoulos D, Glover I, Lemon RN, and Baker SN.** Slowly-conducting pyramidal tract
790 neurons in macaque and rat. *Cereb Cortex* In Press: 2019.
- 791 **Krutki P, Jankowska E, and Edgley SA.** Are crossed actions of reticulospinal and vestibulospinal
792 neurons on feline motoneurons mediated by the same or separate commissural neurons? *J Neurosci*
793 23: 8041-8050, 2003.
- 794 **Kurata K, and Wise SP.** Premotor and supplementary motor cortex in rhesus monkeys: neuronal
795 activity during externally- and internally-instructed motor tasks. *Exp Brain Res* 72: 237-248, 1988.
- 796 **Kurtzer I, Bouyer LJ, Bouffard J, Jin A, Christiansen L, Nielsen JB, and Scott SH.** Variable impact of
797 tizanidine on the medium latency reflex of upper and lower limbs. *Exp Brain Res* 236: 665-677, 2018.

- 798 **Kurtzer IL.** Long-latency reflexes account for limb biomechanics through several supraspinal
799 pathways. *Frontiers in integrative neuroscience* 8: 99, 2014.
- 800 **Landgren S, Phillips CG, and Porter R.** Minimal synaptic actions of pyramidal impulses on some alpha
801 motoneurons of the baboon's hand and forearm. *J Physiol* 161: 91-111, 1962.
- 802 **Lemon RN.** Descending pathways in motor control. *Annu Rev Neurosci* 31: 195-218, 2008.
- 803 **Lemon RN.** Methods for Neuronal recording in Conscious Animals. *Wiley, London* 4: 1-162, 1984.
- 804 **Lemon RN, Baker SN, Davis JA, Kirkwood PA, Maier MA, and Yang HS.** The importance of the
805 cortico-motoneuronal system for control of grasp. *Novartis Foundation symposium* 218: 202-215;
806 discussion 215-208, 1998.
- 807 **Lemon RN, Mantel GWH, and Rea PA.** Recording and identification of single motor units in the free-
808 -to-move primate hand. *Exp Brain Res* 81: 95-106, 1990.
- 809 **Lemon RN, and Porter R.** Afferent input to movement-related precentral neurones in conscious
810 monkeys. *Proceedings of the Royal Society of London, Series B* 194: 313-339, 1976a.
- 811 **Lemon RN, and Porter R.** A comparison of the responsiveness to peripheral stimuli of pre-central
812 cortical neurones in anaesthetized and conscious monkeys [proceedings]. *J Physiol* 260: 53P-54P,
813 1976b.
- 814 **Lewis GN, Polych MA, and Byblow WD.** Proposed cortical and sub-cortical contributions to the long-
815 latency stretch reflex in the forearm. *Exp Brain Res* 156: 72-79, 2004.
- 816 **Lourenco G, Iglesias C, Cavallari P, Pierrot-Deseilligny E, and Marchand-Pauvert V.** Mediation of
817 late excitation from human hand muscles via parallel group II spinal and group I transcortical
818 pathways. *J Physiol* 572: 585-603, 2006.
- 819 **Lundberg A.** Integration in a propriospinal motor centre controlling the forelimb in the cat. *Igaku*
820 *Shoin, Tokyo, New York* 47-65, 1979a.
- 821 **Lundberg A.** Multisensory control of spinal reflex pathways. *Prog Brain Res* 50: 11-28, 1979b.
- 822 **Lundberg A, and Voorhoeve PE.** Pyramidal activation of interneurons of various spinal reflex arcs in
823 the cat. *Experientia* 17: 46-47, 1961.
- 824 **Maier MA, Bennett KM, Hepp-Reymond MC, and Lemon RN.** Contribution of the monkey
825 corticomotoneuronal system to the control of force in precision grip. *J Neurophysiol* 69: 772-785,
826 1993.
- 827 **Marque P, Nicolas G, Simonetta-Moreau M, Pierrot-Deseilligny E, and Marchand-Pauvert V.** Group
828 II excitations from plantar foot muscles to human leg and thigh motoneurons. *Exp Brain Res* 161:
829 486-501, 2005.
- 830 **Marsden CD, Merton PA, and Morton HB.** Human postural responses. *Brain* 104: 513-534, 1981.
- 831 **Matthews PB.** Analysis of human long-latency reflexes by cooling the peripheral conduction
832 pathway; which afferents are involved? *Prog Brain Res* 80: 103-112; discussion 157-160, 1989.
- 833 **Matthews PBC.** *Mammalian muscle receptors and their central actions.* London: Edward Arnold,
834 1972.
- 835 **Matthews PBC, Farmer SF, and Ingram DA.** On the localization of the stretch reflex of intrinsic hand
836 muscles in a patient with mirror movements. *J Physiol* 428: 561-577, 1990.
- 837 **Maxwell DJ, Riddell JS, and Jankowska E.** Serotonergic and noradrenergic axonal contacts
838 associated with premotor interneurons in spinal pathways from group II muscle afferents. *Eur J*
839 *Neurosci* 12: 1271-1280, 2000.
- 840 **McGregor MM, and Nelson AB.** Circuit Mechanisms of Parkinson's Disease. *Neuron* 101: 1042-1056,
841 2019.
- 842 **Mendell LM, and Henneman E.** Terminals of single Ia fibers: distribution within a pool of 300
843 homonymous motor neurones. *Science* 160: 96-98, 1968.
- 844 **Meskers CG, Schouten AC, Rich MM, de Groot JH, Schuurmans J, and Arendzen JH.** Tizanidine does
845 not affect the linear relation of stretch duration to the long latency M2 response of m. flexor carpi
846 radialis. *Exp Brain Res* 201: 681-688, 2010.
- 847 **Miller AD, and Brooks VB.** Late muscular responses to arm perturbations persist during supraspinal
848 dysfunctions in monkeys. *Exp Brain Res* 41: 146-158, 1981.

- 849 **Molander C, and Grant G.** Cutaneous projections from the rat hindlimb foot to the substantia
850 gelatinosa of the spinal cord studied by transganglionic transport of WGA-HRP conjugate. *J Comp*
851 *Neurol* 237: 476-484, 1985.
- 852 **Nathan PW, and Smith MC.** The rubrospinal and central tegmental tracts in man. *Brain* 105: 223-
853 269, 1982.
- 854 **Omrani M, Pruszynski JA, Murnaghan CD, and Scott SH.** Perturbation-evoked responses in primary
855 motor cortex are modulated by behavioral context. *J Neurophysiol* 112: 2985-3000, 2014.
- 856 **Otero JB.** Comparison between red nucleus and precentral neurons during learned movements in
857 the monkey. *Brain Res* 101: 37-46, 1976.
- 858 **Pierrot-Deseilligny E, and Burke DC.** *The circuitry of the human spinal cord : spinal and corticospinal*
859 *mechanisms of movement*. Cambridge: Cambridge University Press, 2012, p. xxiii, 606 p.
- 860 **Pruszynski JA.** Primary motor cortex and fast feedback responses to mechanical perturbations: a
861 primer on what we know now and some suggestions on what we should find out next. *Frontiers in*
862 *integrative neuroscience* 8: 72, 2014.
- 863 **Pruszynski JA, Kurtzer I, and Scott SH.** The long-latency reflex is composed of at least two
864 functionally independent processes. *J Neurophysiol* 106: 449-459, 2011.
- 865 **Pruszynski JA, Kurtzer I, and Scott SH.** Rapid motor responses are appropriately tuned to the metrics
866 of a visuospatial task. *J Neurophysiol* 100: 224-238, 2008.
- 867 **Pruszynski JA, Omrani M, and Scott SH.** Goal-dependent modulation of fast feedback responses in
868 primary motor cortex. *J Neurosci* 34: 4608-4617, 2014.
- 869 **Prut Y, and Fetz EE.** Primate spinal interneurons show pre-movement instructed delay activity.
870 *Nature* 401: 590-594, 1999.
- 871 **Riddell JS, and Hadian M.** Interneurones in pathways from group II muscle afferents in the lower-
872 lumbar segments of the feline spinal cord. *J Physiol* 522 Pt 1: 109-123, 2000.
- 873 **Riddle CN, and Baker SN.** Convergence of pyramidal and medial brain stem descending pathways
874 onto macaque cervical spinal interneurons. *J Neurophysiol* 103: 2821-2832, 2010.
- 875 **Roby-Brami A, and Bussel B.** Long-latency spinal reflex in man after flexor reflex afferent
876 stimulation. *Brain* 110 (Pt 3): 707-725, 1987.
- 877 **Schepens B, and Drew T.** Descending signals from the pontomedullary reticular formation are
878 bilateral, asymmetric, and gated during reaching movements in the cat. *J Neurophysiol* 96: 2229-
879 2252, 2006.
- 880 **Schepens B, and Drew T.** Independent and convergent signals from the pontomedullary reticular
881 formation contribute to the control of posture and movement during reaching in the cat. *J*
882 *Neurophysiol* 92: 2217-2238, 2004.
- 883 **Schepens B, Stapley P, and Drew T.** Neurons in the pontomedullary reticular formation signal
884 posture and movement both as an integrated behavior and independently. *J Neurophysiol* 100:
885 2235-2253, 2008.
- 886 **Shalit U, Zinger N, Joshua M, and Prut Y.** Descending systems translate transient cortical commands
887 into a sustained muscle activation signal. *Cereb Cortex* 22: 1904-1914, 2012.
- 888 **Soteropoulos DS, and Baker SN.** Different contributions of the corpus callosum and cerebellum to
889 motor coordination in monkey. *J Neurophysiol* 98: 2962-2973, 2007.
- 890 **Soteropoulos DS, Williams ER, and Baker SN.** Cells in the monkey ponto-medullary reticular
891 formation modulate their activity with slow finger movements. *J Physiol* 590: 4011-4027, 2012.
- 892 **Stecina K, Jankowska E, Cabaj A, Pettersson LG, Bannatyne BA, and Maxwell DJ.** Premotor
893 interneurons contributing to actions of feline pyramidal tract neurones on ipsilateral hindlimb
894 motoneurons. *J Physiol* 586: 557-574, 2008.
- 895 **Takei T, and Seki K.** Spinal interneurons facilitate coactivation of hand muscles during a precision
896 grip task in monkeys. *J Neurosci* 30: 17041-17050, 2010.
- 897 **Takei T, and Seki K.** Spinal premotor interneurons mediate dynamic and static motor commands for
898 precision grip in monkeys. *J Neurosci* 33: 8850-8860, 2013.

- 899 **Tracey DJ, Walmsley B, and Brinkman J.** 'Long-loop' reflexes can be obtained in spinal monkeys.
 900 *Neurosci Lett* 18: 59-65, 1980.
- 901 **Williams ER, Soteropoulos DS, and Baker SN.** Coherence between motor cortical activity and
 902 peripheral discontinuities during slow finger movements. *J Neurophysiol* 102: 1296-1309, 2009.
- 903 **Williams ER, Soteropoulos DS, and Baker SN.** Spinal interneuron circuits reduce approximately 10-
 904 Hz movement discontinuities by phase cancellation. *Proc Natl Acad Sci U S A* 107: 11098-11103,
 905 2010.
- 906 **Woolf CJ, and Fitzgerald M.** Somatotopic organization of cutaneous afferent terminals and dorsal
 907 horn neuronal receptive fields in the superficial and deep laminae of the rat lumbar spinal cord. *J*
 908 *Comp Neurol* 251: 517-531, 1986.
- 909 **Yang L, Michaels JA, Pruszynski JA, and Scott SH.** Rapid motor responses quickly integrate
 910 visuospatial task constraints. *Exp Brain Res* 211: 231-242, 2011.
- 911 **Yoshino-Saito K, Nishimura Y, Oishi T, and Isa T.** Quantitative inter-segmental and inter-laminar
 912 comparison of corticospinal projections from the forelimb area of the primary motor cortex of
 913 macaque monkeys. *Neuroscience* 171: 1164-1179, 2010.

914

915

916

917

918

919

920 **Figure 1. Schematic of possible circuits to mediate long latency responses to perturbation.** In blue
 921 is a spinal motoneuron, while in gray are three different pre-motoneuronal sources (spinal cord,
 922 brainstem and cortex). The question mark is to highlight the lack of knowledge regarding the
 923 potential role of spinal interneurons to contribute to activity in muscles following a perturbation
 924 despite it being well established that many spinal neurons are in receipt of many afferent and
 925 descending inputs.

926 **Figure 2. Task signals during perturbation and example EMG responses.** A, overlain lever position
 927 traces aligned relative to the perturbation onset. B, velocity traces of expanded epoch around the
 928 perturbation. C, lever acceleration. D, mean rectified EMG signals recorded from the same session.
 929 Calibration bars for each muscle correspond to 10% of the mean EMG pre-perturbation epoch
 930 (100ms).

931

932 **Figure 3. Response incidence in recorded muscles.** A, the incidence of responses for each muscle
 933 across all recording sessions. B, total number of muscles showing a response per recorded session. C,
 934 temporal profile of the response for 1DI across sessions, where each time point shows the fraction

935 of all sessions which had a value larger than $2 \times \text{SD}$ of the background epoch. D, same as C but for the
 936 muscles in the extensor compartment in the forearm. E, same as C but for the muscles in the flexor
 937 compartment in the forearm. For all muscles recorded the response to the perturbation continued
 938 beyond 70ms post-perturbation.

939 **Figure 4. Muscle responses to pyramidal tract (PT) stimulation.** Example rectified EMG responses
 940 from recorded muscles following single shock PT stimulation at $300 \mu\text{A}$ (long grey line). Numbers next
 941 to each response indicate the onset latency of the response in ms (short grey lines).

942 **Figure 5. Estimated response latencies of muscles.** A, mean muscle response aligned to the onset of
 943 the perturbation. EMG responses scaled to the pre-perturbation epoch (100ms). Bottom trace shows
 944 a velocity trace average. Under each muscle trace is the estimated peripheral loop time for each
 945 muscle (triangle, black for monkey D and gray for monkey R); the dots after correspond to response
 946 latencies for the given muscle measured from individual recording sessions. B, histogram of the
 947 response latency for each muscle aligned relative to the peripheral loop time for the given muscle.
 948 The bottom plot is a similar histogram combined across all muscles.

949 **Figure 6. Example responses in spinal interneurons.** A, average position (top) and velocity (bottom)
 950 traces for a single recording session. Arrow indicates the direction of movement that causes a finger
 951 extension. B, the peri-event time histogram for three cells recorded from the spinal cord (in red)
 952 overlain on the corresponding raster plots. Horizontal dotted line indicates the pre-perturbation
 953 firing rate.

954 **Figure 7. Response incidence in the spinal cord.** A, pie chart showing the fraction of spinal
 955 unidentified (UID) cells responding to the perturbation with an increase in rate (red), a decrease
 956 (blue) or no response (black). The raster to the right of the pie chart shows the bins for each neuron
 957 that were larger (in red) or smaller (blue) than twice the standard deviation of the pre-perturbation
 958 epoch (100ms). Cells have been sorted by response latency. B, same as A but for identified spinal
 959 pre-motor (PM) cells. C, mean PETH across all spinal cells. In red is the mean response across all cells
 960 with a positive response, in blue for those with a negative response and in black is the mean for
 961 those with no significant response. Baseline activity has been subtracted from each cell prior to
 962 averaging. D, depth distribution of all recorded spinal cells. In grey are the UIDs and in black are the
 963 PM cells. The red trace shows a sliding average of the fraction of cells at a given depth that
 964 responded to the perturbation. E, depth distribution of cells responding to cutaneous stimulation
 965 (black) and to deep stimulation (grey). F, depth distribution of cells responding to cutaneous
 966 stimulation in the hand (black line), and those that also responded to the finger perturbation (red
 967 line).

968 **Figure 8. Response incidence in the primary motor cortex.** A, pie chart showing the fraction of M1
 969 unidentified (UID) cells responding to the perturbation with an increase in rate (red) or a decrease
 970 (blue) or no response (black). The raster to the right of the pie chart shows the bins for each neuron
 971 that were larger (in red) or smaller (blue) than twice the standard deviation of the pre-perturbation
 972 epoch (100ms). Cells have been sorted by response latency. B, same as (A) but for identified PTNs. C,
 973 same as (A) but for identified CM cells. D, mean PETH across all M1 cells. In red is the mean response
 974 across all cells with a positive response, in blue for those with a negative response and in black is the
 975 mean for those with no significant response. Baseline activity has been subtracted from each cell
 976 prior to averaging.

977 **Figure 9. Baseline firing and response magnitudes in M1 and SC.** A, boxplots of baseline firing rates
 978 for the different cell types indicated on the x-axis. Only cells with no significant response to the
 979 perturbation are used. The same color code applies to remaining panels. B, same as (A) but for cells
 980 that responded to the perturbation. C, absolute magnitude of the responses (relative to baseline, in
 981 spikes/s) for each cell type. For the purposes of this plot, the absolute value of response was used,
 982 such that cells with rate suppressions contribute positive values to the population. D, signal to
 983 background ratio (SBR), formed by dividing the response magnitude of (C) by the baseline rate in (B)
 984 for each cell type; note the logarithmic scale. UID, unidentified cells in either M1 and SC, PTN,
 985 identified pyramidal tract neurons, CM, M1 cortico-motoneuronal cells; PM, pre-motoneuronal cells
 986 in the SC. * corresponds to a significant difference ($P < 0.01$).

987 **Figure 10. Response onset latency distribution.** A, cumulative distribution of response latency
 988 following perturbation for SC cells (gray) and PTNs from M1 (black). The distributions were
 989 significantly different between areas (two-sample Kolmogorov-Smirnov test, $p < 0.0013$). B,
 990 distribution histogram of response latency for the different cell types. Dotted line marks 10 ms
 991 latency for reference throughout.

992 **Figure 11. Exemplar spinal premotor neuron responding to index finger perturbation.**

993 A1, Waveform traces from 10 mechanical perturbations. The red circles highlight the action
 994 potentials of this given cell. Note that more than one cell was present in the recordings. A2, mean
 995 response of 1DI muscle for same trials which the cell was presynaptic to. EMG activity was
 996 normalized relative to pre-perturbation levels. A3, mean velocity trace of lever. B, same as A but for
 997 all trials that this cell was recorded from. Red arrow indicates onset of neural response and black
 998 arrow indicates onset of 1DI response. The time axis is the same for all subplots.

999

Figure 12. Estimation of sensorimotor loop time for a cell with direct linkage to motoneurons. A, simplified schematic demonstrating the ‘transcortical’ loop for a CM cell following a sensory perturbation, through cell activation and back to muscle. A similar schematic would apply for PM cells. For simplicity the afferent component is depicted as a single link but the dotted line indicates that this is a polysynaptic path (for M1), or could be a mono- or polysynaptic path (for SC). B, delay from perturbation to cell response for a CM cell in M1(t_{sensory}). The top trace is the PETH for the given cell and underneath are the mean velocity and acceleration traces. For this particular cell the onset latency was 26.5ms. C, delay from cell to muscle, estimated through spike-triggered averaging (t_{motor}). The top trace is the trigger pulse from spike detection and the lower trace is the average for the target muscle for this cell (1DI). In this example, the STA latency is 9.1ms. D, EMG response of target muscle to the perturbation, with onset and offset demarcated by dotted lines. The grey bar indicates the response epoch for this muscle and the red and green arrows indicate the estimated delays from (B) and (C) respectively. Their sum is the loop time (35.6ms) for this particular neuron (indicated by the dotted line); this is the earliest time at which the response of this cell to the perturbation could start making a contribution to the response of the target muscle.

Figure 13. Population loop times for pre-motoneuronal cells. A, distribution of loop delays (sum of efferent delay and response delay to perturbation), compared to the onset and duration of muscle response which cells were pre-synaptic to. In red are CM cells from M1 and in cyan are PM cells from the SC. The grey boxes correspond to the duration of the EMG response for the target muscle (truncated at 100ms post perturbation). B1, mean EMG response across effects shown in A. EMG was normalized as a fraction relative to pre-perturbation epoch. B2, histogram of loop times for CM (red) and PM (cyan) cells. C, histogram of loop times expressed relative to EMG response onset. Same color codes as A. Negative values indicate cell responses prior to EMG onset. The EMG responses were also aligned relative to their onset and the grey line shows the fraction of effects responding at any given time after EMG response onset. As EMG responses had varying durations (as shown in A), the fraction decreases with time.

Figure 14. Relative responsiveness of M1 and SC. A, fraction of responsive cells in each area (M1 PTNs: red, SC: cyan) that are active post-perturbation. B, ratio of the response fraction between the two areas ($RespR$, Eq 1), plotted on a logarithmic scale. The dotted lines show the 95% confidence limits. PETHs were shifted according to their antidromic latencies before the curve for M1 was compiled. All times post-perturbation are therefore for activity reaching the spinal level. There are two epochs of significant difference (11-21ms and 35-41ms; grey shading) with two additional brief crossings of the confidence limits (between 80 and 90ms) highlighted by the small triangles. C, same as (A) but only using spinal PM cells. D, same as B, showing three epochs of significant difference

1034 between areas (14-17ms, 35-41ms, 88-93ms). E, fraction of EMGs with significant activity. EMG
1035 response timings were shifted by subtracting the corresponding efferent delay for each muscle,
1036 thereby aligning EMG responses relative to the neural activity at the spinal level. Axis is thus the
1037 same as for (C, D). The triangles show the actual time of perturbation for the EMG traces. Muscle
1038 responses were grouped to 1DI (blue), muscles from extensor (Ext, green) and flexor (Flex, red)
1039 compartments in forearm.

1040 **Figure 15. Comparison of Response Latency in M1 and SC.** A, cumulative distribution of response
1041 latency following perturbation for all SC cells (cyan) and PTNs (red). PTN latencies were adjusted to
1042 include the conduction delay from cortex to spinal cord based on the PTN-specific antidromic
1043 latency. The two distributions are significantly different (two-sample Kolmogorov-Smirnov test,
1044 $p < 0.001$). Vertical dotted lines indicate fraction of SC cells with latencies smaller than fastest and
1045 second-fastest PTN. B, percentile plot showing the percentage of SC cells with latencies smaller than
1046 a given percentage of PTN cells (thick black line). Thin black line shows the percentage of SC cells
1047 with latencies smaller than a percentage of PTN cells, plus spinal cells from the superficial layers of
1048 the spinal cord (depth < 0.5 mm) that are known not to receive any direct PT inputs.

1049 **Figure 16. Directionality index during task.** A, top trace shows PETH for example cell during flexion
1050 (blue) vs extension (red) trials. Bottom trace shows the directionality index (DI) for the same cell –
1051 note the high DI values during the movement part of the task. B, same as A, but for a different cell
1052 with a lower DI as the cell responds very similarly during the two trial types. C, mean lever position
1053 signals for flexion (blue) and extension trials (red). The maximal lever angle corresponds to the finger
1054 being flexed. D, distribution of DI values for M1 (black) and SC cells (grey). E, boxplots showing the
1055 median DI (with 25th and 75th percentiles outlined by box) during the task for M1 (black) and SC cells
1056 (grey), divided into the population of cells that responded to the perturbation (Pert+) and those that
1057 did not (Pert-).

1058

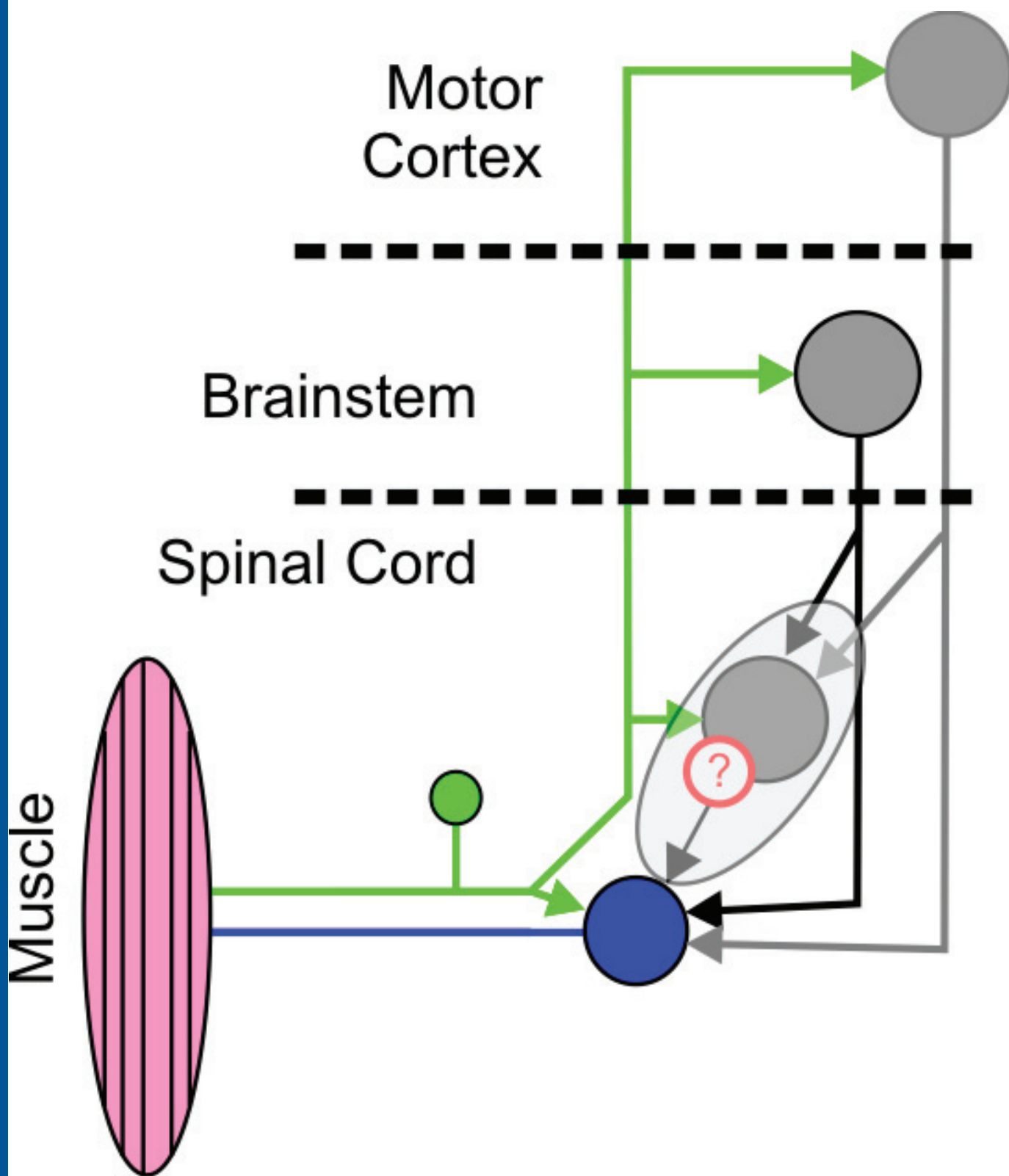
1059

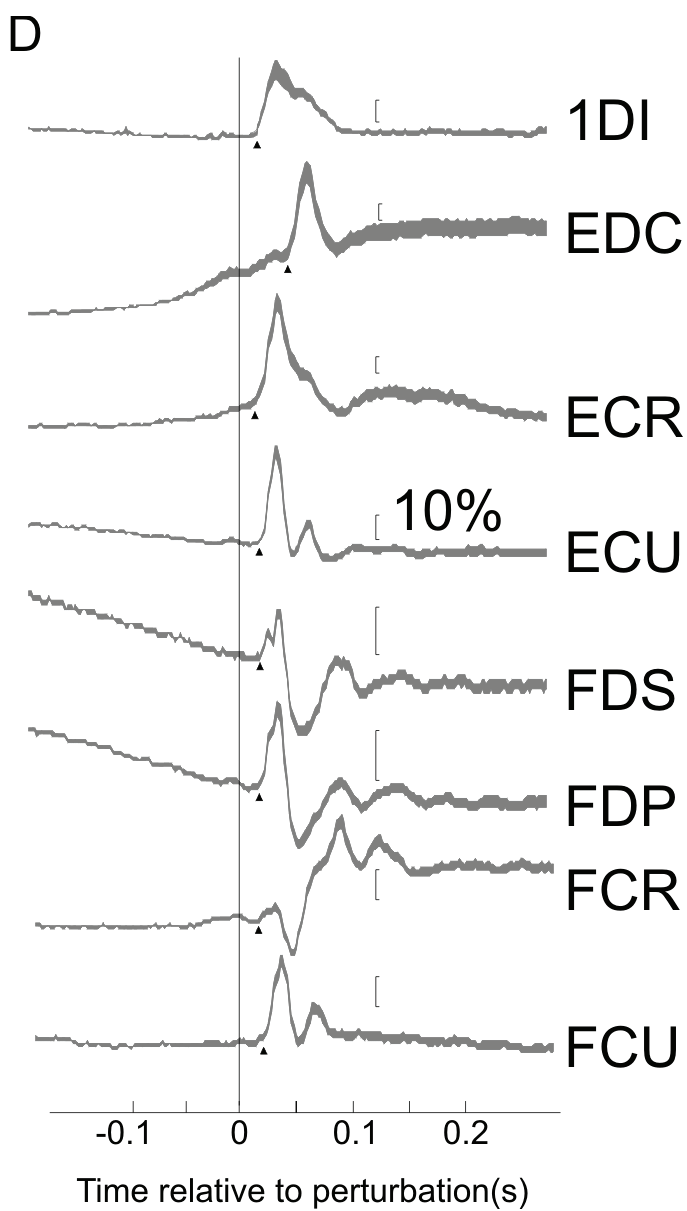
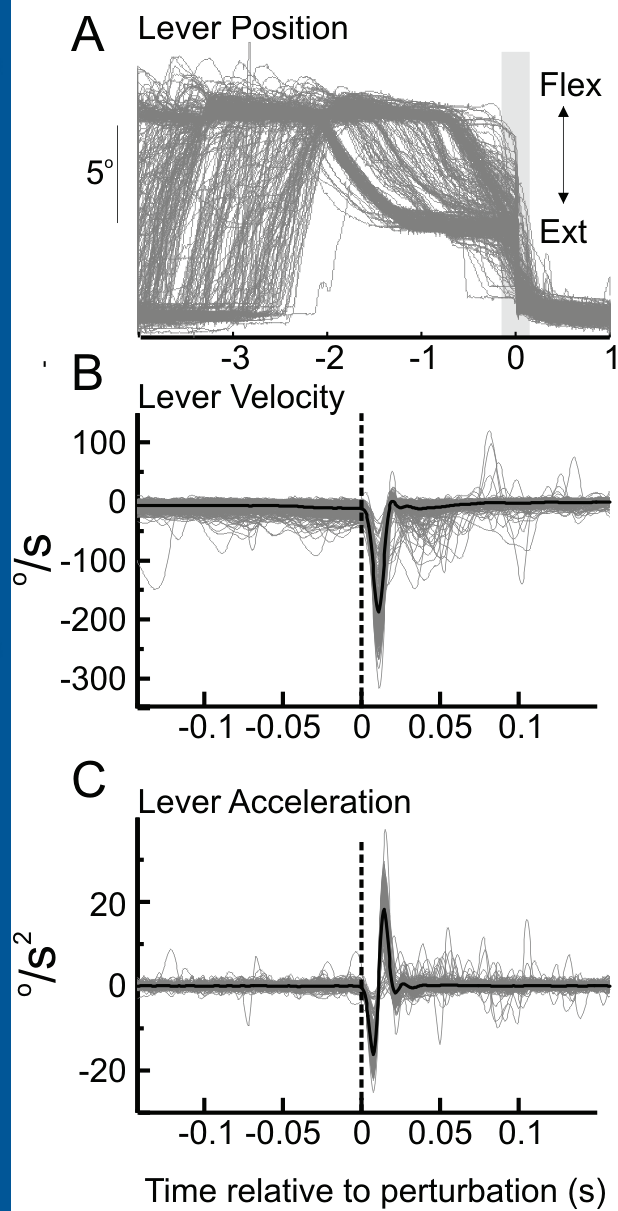
1060

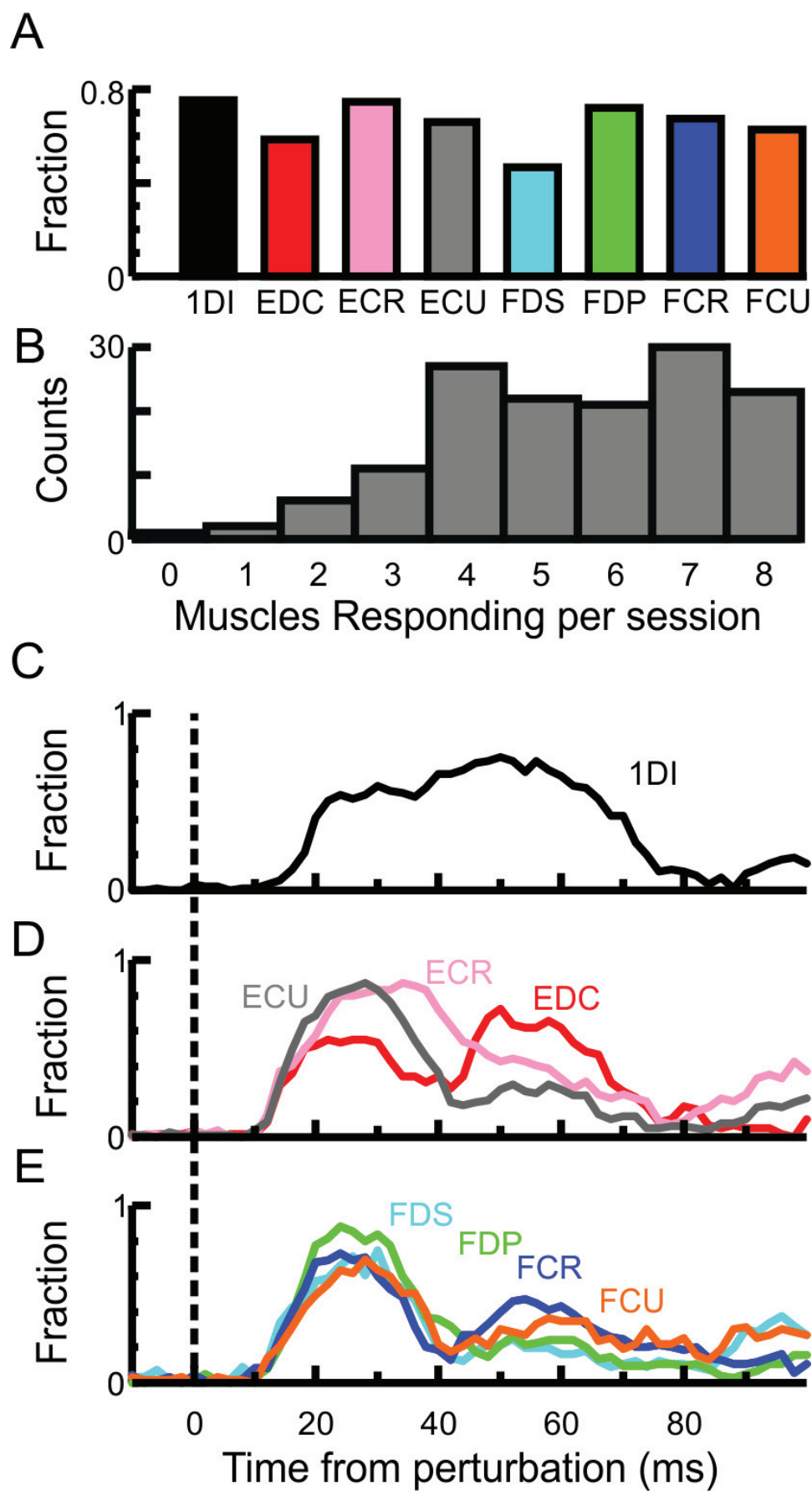
1061

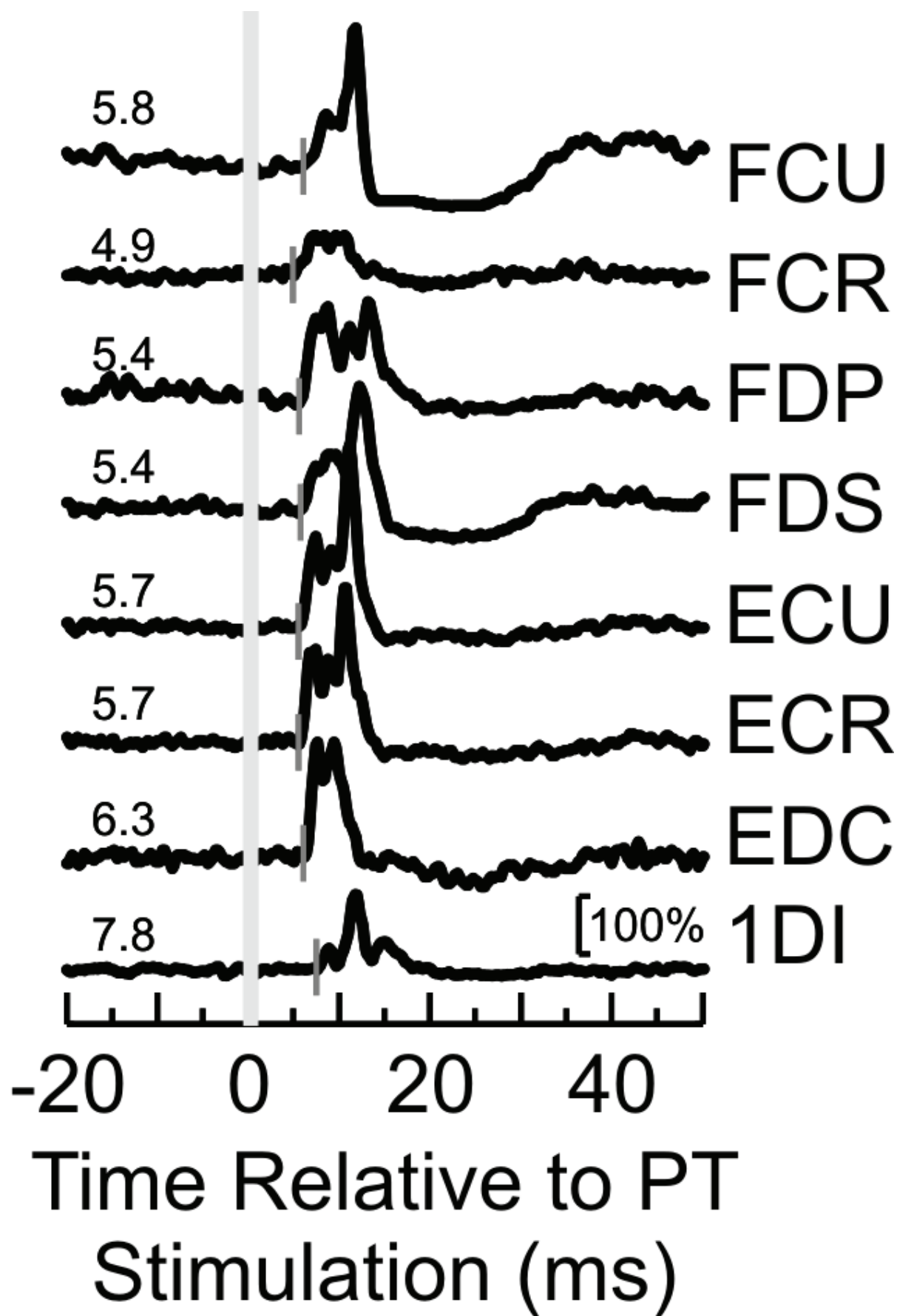
1062

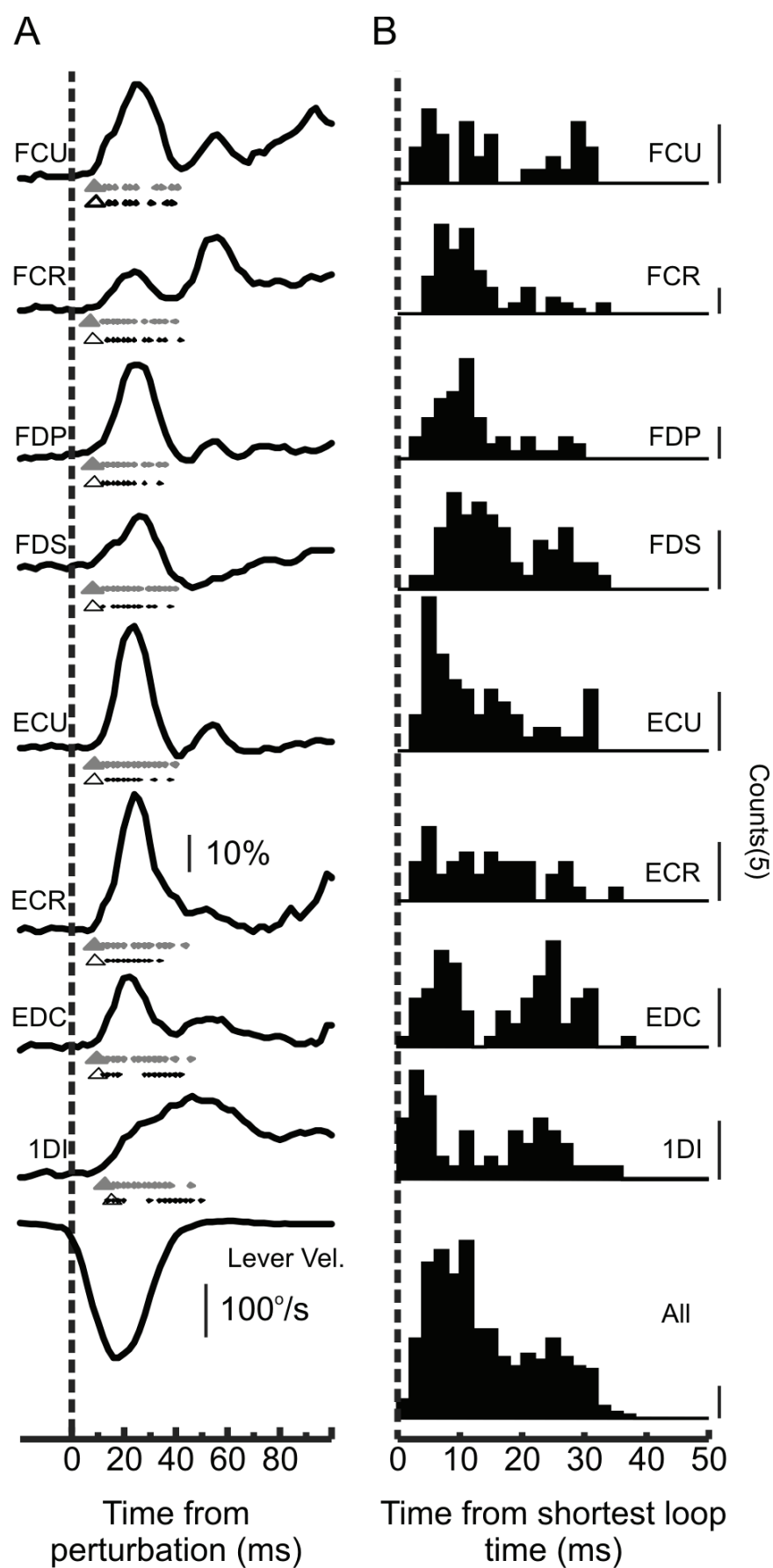
1063



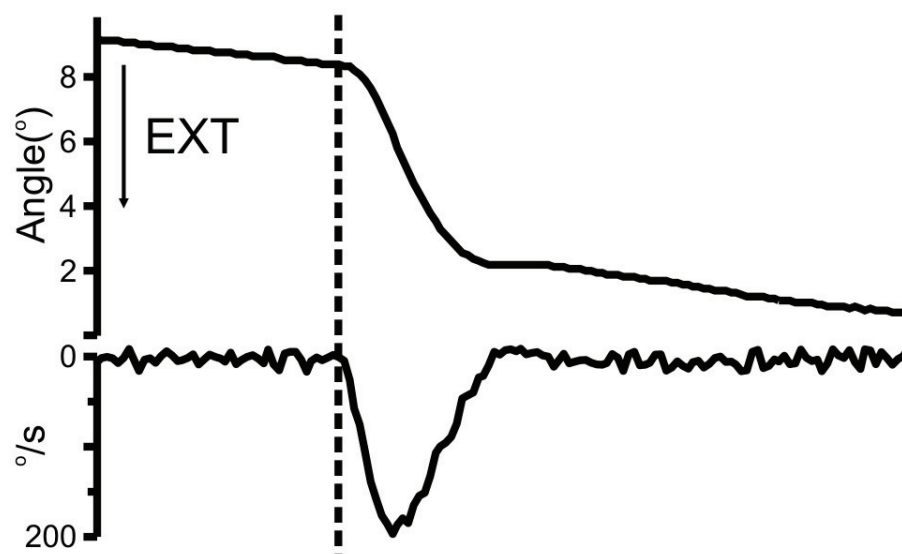








A



B

